Alma Mater Studiorum · Università di Bologna

School of Science
Department of Physics and Astronomy
Master Degree in Physics

Electroweak Sudakov corrections for processes at a future Muon Collider

Supervisor:
Prof. Davide Pagani

Co-supervisor:
Prof. Marco Zaro

Submitted by:
Antonio Sandroni

Academic Year 2021/2022

Abstract

Precision calculations are crucial for the validation or falsification of our understanding of fundamental interactions at colliders. One relevant aspect for present and future colliders is the impact of effects coming from electroweak (EW) corrections. In this thesis, we study the structure of the so-called virtual Electroweak Sudakov logarithms, which are the dominant contribution of EW higher-order corrections in the high-energy regime. In particular, we investigate the phenomenological impact for production processes at a future high-energy muon collider, for which EW Sudakov logarithms are expected to be very large. After reviewing the structure of the Denner and Pozzorini (DP) algorithm for the calculation of EW Sudakov logarithms, and its recent revisitation in the literature, we (re)produce results for a proton–proton machine at 100 TeV. Then we consider the case of a muon collider at 3, 10 and 30 TeV. We therefore comment the results obtained for relevant representative processes, and we discuss the phenomenological differences with respect to the proton–proton machine. Finally, we study the partial cancellations induced by the Heavy-Boson-Radiation (HBR) at a high-energy muon collider. In the thesis, we show several numerical results for both differential and inclusive cross sections, which we have produced with the help of the MadGraph framework.

Contents

Chapter 1

Introduction

Colliders are meant to find radically novel knowledge about the fundamental structure of particles and their interactions. By increasing the energy of the collisions, not only it is possible to study new physics phenomena at smaller and smaller distances, but also new unobserved particles can be in principle directly produced. In order to study new physics, an alternative approach, which so far has been shown to be complementary and equivalently valid, is what is commonly called precision physics. By measuring with very high precision the properties of particles that we have already discovered, namely those that are part of the Standard Model (SM) of particles physics, it is possible to detect (or exclude) the indirect quantum effects from possible new particles or interactions Beyond-the-SM (BSM).

So far, all colliders, including the Large Hadron Collider (LHC), have not observed any clear and unambiguous sign of BSM physics. Recently, a different option as future collider has been (re)proposed: a high-energy muon collider. The interest in such a collider is easily explained. Muons, as electrons and positron, allows performing several precision studies, but unlike electrons and positron they can be accelerated at much higher energies due to the lower energy loss via synchrotron radiation. Moreover, at variance with the hadronic counterpart, in muon collisions the total energy of the collider is available to produce the scattering process

In order to detect possible signs of BSM physics and perform precision-physics studies, we need to have under control everything that concerns the SM. In perturbative calculations, electroweak (EW) corrections are paramount in this context, especially in the case of two colliding leptons, as the muons. In this thesis we study a particular feature of them, the so called EW Sudakov enhancements or Sudakov logarithms, which induce large and negative corrections to the cross section. Moreover, in a high energy regime, EW Sudakov logarithms are a very good approximation of the exact result at one-loop accuracy, namely the Next-to-Leading (NLO) EW corrections, as we will discuss in the thesis, and their evaluation is much faster and stable of the NLO EW. Therefore, their precise evaluation opens up several possibilities, among which, e.g., the automation of the resummation of EW Sudakov logarithms matched to the NLO EW result.

In the thesis we will exploit the tool MadGraph, an event generator based on Monte Carlo methods, for simulating muon collisions. MadGraph is capable of handling computation of leading-order (LO) and NLO cross sections in a unified framework with a

high level of flexibility. Also, both exact NLO EW corrections and their Sudakov approximation can be calculated.

In the rest of this section, we will review the ideas that have led to the formulation of the SM and the basics ideas related to the cross section as a fundamental concept for studying Quantum Field Theory at colliders. We will also review the relevance of colliders and motivate why a high-energy muon collider is an intriguing option for the future. In section 2 we will then discuss the structure of the Denner and Pozzorini (DP) algorithm for the calculation of EW Sudakov logarithms, and its recent revisitation and implementation in MadGraph. In section 3 we will present the results obtained and we will comment their phenomenological features. First we will look at the case of a proton–proton machine at 100 TeV, and then we will consider the case of a muon collider at 3, 10 and 30 TeV. We will comment the results obtained for relevant representative processes, and we discuss the phenomenological differences with respect to the proton–proton machine. Finally, we will also study the partial cancellations induced by the Heavy-Boson-Radiation (HBR) at a high-energy muon collider.

1.1 The Standard Model

The Standard Model is a theoretical framework that describes the fundamental particles and interactions in particle physics. Today it is the most precise and accurate model to describe three of the four fundamental forces of nature: the electromagnetic force, the weak force, and the strong force.

- Strong Force: is the strongest force of the four, responsible for holding the nucleus together, binding protons and neutrons.
- Weak Force: is responsible for the radioactive decay.
- Electromagnetic Force: is responsible for the attraction between charged particles and has an infinite range of action.
- Gravity: is responsible for the attraction between massive objects. It has an infinite range of action and is the only force not included in the description Standard Model.

The construction and completion of the Standard Model has been made in so many years, starting in the 1970s, when the works of Glasgow and Salam brought to the unification of the electromagnetic and weak force, up to the discovery of the Higgs boson at LHC (Large Hadron Collider) in 2012, the last piece to complete the landscape of fundamental particles. The theory is based on the fact that all matter is made up of particles called quarks and leptons, which interact with each other through the exchange of force-carrying particles called gauge bosons. The main division of the particles belonging to SM is in two classes: fermions and bosons.

Fermions

Fermions are particles with spin $\frac{1}{2}$, described by Fermi-Dirac statistics, and are of two categories: quarks and leptons. Quarks are governed by the strong force, and are the building blocks of protons and neutrons, which are the particles that make up the nuclei of atoms. There are six flavors of quarks, known as up, down, charm, strange, top, and bottom, and each has a corresponding antiparticle with opposite charge. Leptons are particles that do not interact via the strong force but through electroweak one, and they include these flavors: electron, muon, tau, and their corresponding neutrinos. Like quarks, each lepton has a corresponding antiparticle with opposite charge. The interactions between fermions are mediated by three of the four fundamental forces of nature: the electromagnetic force, the weak nuclear force, and the strong nuclear force.Leptons, as said, do not interact via the strong force and neutrinos do not interact neither via strong not electromagnetic force, but via the weak one.

Bosons

Bosons are the particles responsible for carrying fundamental forces. They are the other main type of particles in the Standard Model, alongside fermions and, unlike these, bosons have integer spin, 0 or 1, which means they can occupy the same quantum state according to their statistics. There are several types of bosons:

- Photons: these are the particles that carry the electromagnetic force, which is responsible for the behavior of electrically charged particles.

- $W^{\pm}$ and Z bosons: these are the particles that carry the weak force.
- Gluons: these are the particles that carry the strong force, which is responsible for holding quarks together to form protons and neutrons.
- Higgs boson: this is the particle associated with the Higgs field, which gives mass to particles.

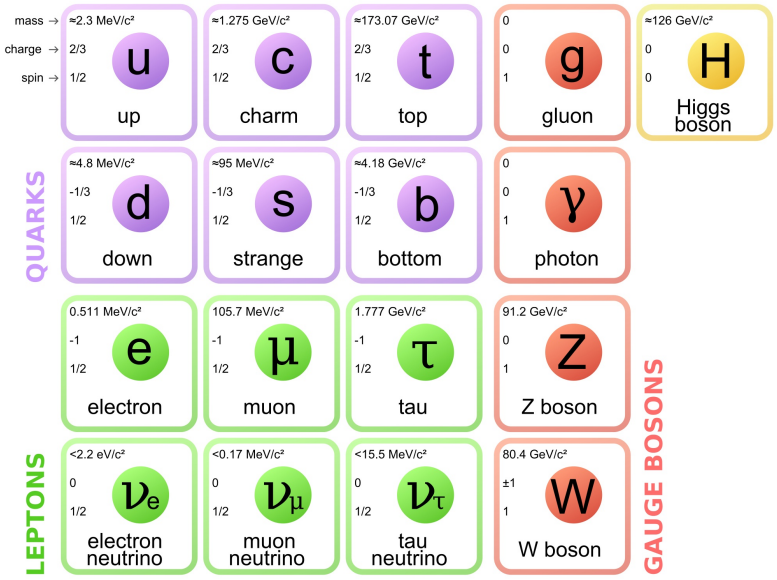

Figure 1.1: All the fundamental particles of Standard Model and their main features, mass, charge, and spin.

We see in Fig.(1.1) that leptons have integer electric charge, 0 for neutrinos and -1 for the other leptons and quarks have a fractional charge. Important discoveries related to the Standard Model were made all along the 20^{th} century, like the discovery of the charm quark in the early 1970s and the one of the bottom quark in that same decade, up to the 1995 when, at Fermilab, the top quark was discovered, bringing further corroboration to the theory's predictions about the existence and properties of these particles.
Quarks also carry color charge, and because of this, they form in nature bound colorless states, called hadrons, that are divided in two different groups according to their composition: baryons, triplet of quarks like the protons and the neutrons that build up the atoms of nuclei, and mesons, made by pairs of quarks.
The interactions between bosons and fermions regulate the behavior of matter in the universe. For example, the electromagnetic force between particles is mediated by the exchange of photons, while the strong nuclear force between quarks is mediated by the exchange of gluons. In the SM, the electromagnetic force, is described by Quantum Electrodynamics (QED), which is one of the most successful and well tested physical theories. The quantum particles that mediate the interaction is the photon, massless and with spin 1, that allows the interaction to have an infinite range of action; this force decreases with the increasing of the distance, being inversely proportional to the square of it, and proportional to the QED coupling constant α, with usually the value of $\frac{1}{137} \simeq 0.01$.
Differently from QED, the weak interaction is mediated by three charged massive bosons: W^+, W^- for charged current interactions and Z for neutral current interactions. Their

mass is in accord with the short distance of the weak force. These forces were unified in the decade across the 1970s and the 1980s thanks to the work of Glasgow, Salam and Weinberg, all rewarded with the Nobel Prize in 1979. The unification of electromagnetic force and weak one is described by ElectroWeak force, that describes the interactions mediated by gauge bosons between particles that are electrically charged and weakly interacting, such as the electron, the muon, and the tau particle and postulates that the weak force and the electromagnetic force are different manifestations of the same underlying force.
The theory that describes the strong interaction between colored quarks and gluons is the Quantum Chromodynamics (QCD). According to this theory, the strong force is mediated by gluons, discovered by the DESY laboratory in Germany in 1979. One of the key features of QCD is asymptotic freedom, which means that at high energies, the strength of the strong force decreases, allowing quarks and gluons to move relatively freely, in contrast to the behavior of the electromagnetic force, which gets stronger at shorter distances. This peculiarity of QCD, that confines quarks in small regions of space, an effect called confinement, is responsible for the creation of bound states such as hadrons at low energies.
One of the most important discoveries related to the Standard Model is the discovery of the Higgs boson. This discovery was made by the Large Hadron Collider (LHC) at CERN in 2012. The Higgs boson was first proposed in the 1960s as part of the Standard Model, but it took nearly 50 years to confirm its existence. Its discovery was important because confirmed the mechanism by which particles acquire mass, which is a key feature of the Standard Model. The Standard Model also predicts the existence of a particle called the neutrino, which is an electrically neutral particle that interacts only weakly with other matter. Neutrinos are produced in the Sun and are present in cosmic rays, and they are difficult to detect because they interact only via the weak force with other matter. In 2002, the Sudbury Neutrino Observatory (SNO) in Canada announced the first direct evidence that neutrinos have mass.

The Standard Model has been tested and validated by many experiments over the years, but there are still some unanswered questions and unsolved problems. For example, the theory does not include gravity, which is one of the four fundamental forces of nature. Also, the theory does not explain why there is more matter than antimatter in the universe. In conclusion, the Standard Model is a highly successful theory that describes the fundamental particles and their interactions. It has led to many important discoveries related to particle physics, including the discovery of the Higgs boson, the top quark, and the neutrino. However, there are still many unanswered questions and challenges that remain to be addressed in our understanding of the Universe

1.2 Cross section

In this section we will review the concept of cross section, central in collider physics, and how it is generally calculated at various orders of precision. This will allow us to see where and why the so called Sudakov logarithms enter the game, as we will explain in the following chapter.
Cross section is a quantity measured experimentally that gives the probability for a specific process to happen; considering a beam of particles, of fixed number density and velocity, hitting a certain target, we can build the cross sectional area of the target

$$\sigma = \frac{1}{T\Phi} N, \tag{1.1}$$

with N the number of particles scattered, T the time for the experiment and Φ the flux of incoming particles (Φ=number density x velocity of the beam), where the flux and time are experiment dependent, and the number of interaction is determined by the short distance interactions between particles.

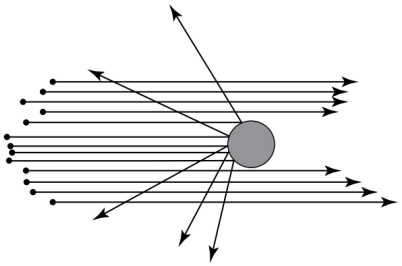

Figure 1.2: Representation of a classical scattering

If in a classical collision, the interaction happens either or not, as sketched in Fig.(1.2) and Eq.(1.1) can be interpreted as the area of the target that interacts with the incoming beam, in the shift to Quantum Mechanics and Quantum Field Theory, the interaction is governed by probability. The classical differential probability of scattering in an experiment of beam collision on a target is

$$P = \frac{N}{N_{inc}}, \tag{1.2}$$

with N the number of particles scattered and N_{inc} the number of incident particles. The cross sectional area in a Quantum Mechanical context is called cross section

$$d\sigma = \frac{1}{T\Phi} dP, \tag{1.3}$$

and is not correspondent to the area of the target but can still, in the same interpretation, more generally viewed as a quantification of the interaction strength between the colliding particles.
In quantum mechanics, states are the fundamental entities to describe the configuration of a system. Consider a scattering experiment in Heisenberg picture, where we have a state $|i\rangle$ to describe the configuration of the state before the scattering, and $|f\rangle$ the final state after the scattering occurred; in Heisenberg picture the final state results from the evolution of the initial state $|i\rangle$ through the evolution by the scattering matrix S that

encapsulates the information about the scattering itself. In the new context of quantum mechanics, the measurable quantities are probabilities, given by the modulus squared of the inner product of states $|\langle f|i\rangle|^2$; the previous classical differential probability of interaction now has this form

$$dP = \frac{|\langle f|S|i\rangle|^2}{\langle f|f\rangle\langle i|i\rangle} d\Pi, \tag{1.4}$$

with $d\Pi$ is the phase space region of momenta of final particles. In a nontrivial process one can focus on computing just the nontrivial part of the S matrix, meaning the part that actually contributes to the scattering, basically

$$|\langle f|S-1|i\rangle| \propto |\langle f|\mathcal{M}|i\rangle|. \tag{1.5}$$

Combining these results, the general form of the total cross section for a process in Quantum Field Theory calculations is

$$\sigma \propto \int |\mathcal{M}|^2 \, d\Phi, \tag{1.6}$$

with the integration made on the phase space of final particles; $\mathcal{M}$ is called the amplitude of the process and contains all the information about the scattering and, when perturbation theory holds, introducing e.g. a parameter as α, it can usefully be expanded as such

$$\mathcal{M} = \mathcal{M}_0 + \alpha\mathcal{M}_1 + \alpha^2\mathcal{M}_2 + ... \tag{1.7}$$

according to the various contributions of different order. For the calculation of cross section we need $|\mathcal{M}|^2$ that, including two orders of contributions, results in

$$\sigma \propto |\mathcal{M}|^2 = \Big|\sum_{i=0}^{\infty} \alpha_i \mathcal{M}_i\Big|^2 = \tag{1.8}$$

$$= |\mathcal{M}_0|^2 + 2\mathfrak{Re}(\alpha\mathcal{M}_0\mathcal{M}_1^\dagger) + \mathcal{O}(\alpha^2) + ... \tag{1.9}$$

The content of the $\mathcal{M}_0$, called Born amplitude, consists of the terms that contributes to the calculation of the cross section at leading order, σ_{LO}, also called tree-level approximation; in calculating σ_{NLO} one has to include other terms: in addition to the tree level contribution, we need to consider the presence of relevant 1-loop diagrams, contained in $\mathcal{M}_1$ that interfere with the terms of order α. Diagrammatically, one can

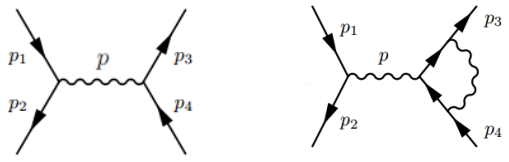

Figure 1.3: Two diagrams contributing to LO (only the first) and NLO (the first and the second) in perturbative expansion for $\mu^+\mu^- \to e^+e^-$ process. The two incoming muons have momentum p_1,p_2, the outgoing electron and positron p_3,p_4, with p the momentum in the s channel.

represent the various contributions trough Feynman diagrams; consider the EW process

$\mu^+\mu^- \to e^+e^-$, the content of $\mathcal{M}_0$ is represented by the left graph in Fig.(1.3) with a photon or a Z boson in the s channel. In the $\mathcal{M}_1$ term, are present, between many, diagrams like the right one of Fig.1.3 with a photon or Z boson in the s channel and in the loop. When loop terms interfere with themselves, they contribute at even higher order, as shown in Eq.(1.9).

In addition to loop corrections, one also needs to calculate real emission graphs be-

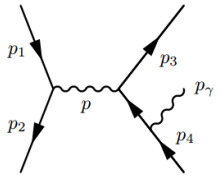

Figure 1.4: Diagram for the real emission of a photon in $\mu^+\mu^- \to e^+e^-$ process. The two incoming muons have momentum p_1,p_2, the outgoing electron and positron p_3,p_4 and the photons p_γ

cause, it is impossible to tell whether the final state in a scattering process is just a particle or that particles plus an arbitrary number of soft or collinear photons, and in the calculation of physical observables one has to take this in consideration. These real emission terms correspond to processes of the same order in perturbation theory, but with one more final particle (see Fig.(1.4)). They are also crucial in the elimination of IR divergences, because if one considers just the loop diagrams, when a massless particle is involved in it, this results in divergences of the cross section value; if one assign a finite mass to the massless particle, the sensitivity to IR divergences comes out with the presence of logarithms in the cross section formula. These logarithms are very large and are the so called Sudakov logarithms that come in to play in electroweak corrections.

The birth of Sudakov logarithms, as we will see, comes from the need to approximate, for high energies, the amplitude, and the cross section calculations, indeed in the term $\mathcal{M}_1$ appear loop diagrams that, when evaluated in computer calculations, imply a heavy work of numerical integration. The approximation made by Sudakov allows keeping, order by order, terms of this form

$$-\alpha^n \log^k(\frac{s}{M_W^2}), \tag{1.10}$$

with n the order of the expansion term kept, k in the range $1 \leq k \leq 2n$ and α the parameter of the expansion.

These logarithms have a physical significance, and they involve, at high energies, two different scales, the W-boson mass M_W and the center of mass energy $\sqrt{s}$. In theories like QCD or QED, theories where the carrier bosons are massless, virtual and real terms in perturbative corrections are separately divergent, and divergences cancel when combined in the physical cross section. If the bosons are massive, on the other hand, there is, in principle, no need to include real emissions as the virtual amplitude is finite. Indeed, the boson mass regulates the divergence. However, if we are in a configuration near the massless limit, for which the boson mass is much smaller than the process energy, the remaining of the divergence appears as terms containing $\log^k(\frac{s}{M_W})$,with $k = 1, 2$. These terms are the so called Sudakov logarithms. When real emissions are included, we know that in EW case there is not a perfect cancellation of these kinds of divergences and that

they result in logarithmic terms that indicate the sensitivity to IR divergences, so the corrections became relevant, especially in the tails of the distributions; in this work we will see quantitatively this fact. We will see the effects of Sudakov corrections at a muon collider, and we will see, adding the contribution of the emission of a Z boson (Heavy Boson Radiation) the already known fact of partial cancellation between virtual and real part in EW calculations [7].

Even if the computation of the exact NLO EW is technically more involved than the virtual Sudakov logarithmic approximation, only the former was automated in the first place. Thanks to the pioneering work [1] and following improvements proposed, like in [2], has been possible the implementation to calculate both single and double one-loop virtual EW Sudakov logarithms, the typical dominant subclass of NLO EW corrections, at $\mathcal{O}(\alpha)$ in an automated way with MadGraph.
Because they can be calculated analytically via tree-level amplitudes only and because of their dominance and their much faster evaluation respect to the exact $\mathcal{O}(\alpha)$ result, the implementation lead to a very good and fast approximation of NLO EW corrections at high energy. In addition, the Sudakov contribution depends only on the properties of the external particles (masses, momenta, helicities, charges, hypercharges) so can be easily generalized to the BSM case.

1.3 Collider physics

Now we briefly review the history of particle accelerators and colliders to better understand why a muon collider could be a good candidate in taking the place of the machines up to now used. The history of particle colliders is more than 100 years long, starting in the 19^{th} century with the first experiments by Ferdinand Braun and its Cathode ray tubes; from the early discoveries of X-rays in 1895,the electron measurements by Thompson in 1897 and the investigations about the atom nuclei by Rutherford in 1911, these machines have been improved with technological novelties to become more and more efficient. The main purpose of such machines was, from the very beginning, to let us investigate the structure of matter, to see what is inside it and what is made of. The first goal of the developments in this field were in reaching always higher energies; for a long time this has been the main goal and all the efforts in this direction led, through all 20^{th} and 21^{th} century, to the construction of the Standard Model of particles. The discoveries that brought a complete image of the SM were performed in different kinds of particle accelerators, with collisions happening between particles like proton-proton, electron-positron and electron-proton, for the deep inelastic scattering (DIS).
In 1974 the charm quark was discovered at the same time in two laboratories in the United States, on the West Coast at SLAC (Stanford Linear Accelerator Center), a linear electron-positron collider long around 3.2 km and working up to 50 GeV, and in Brookhaven National Laboratory on the East Coast, a circular proton-proton collider that can reach up to 250 GeV. This discovery brought a big support to the theory of QCD. In the following years, the landscape of research in physics would be filled with new particles discovery. At Tevatron, a circular proton anti-proton machine long 6.3 km and working at 1 TeV, situated at Fermilab, was discovered the bottom quark in 1977 and the top one in 1995. With time higher and higher energies have been reached, today at LHC (Large Hadron Collider) the highest energy regime that has ever been explored in a collider experiment has been reached, 13 TeV, bringing the discovery of the Higgs boson in 2011-2013.
This need of reaching higher energies is what is generally referred to as "Energy Frontier". The energy frontier is constantly being pushed forward as new colliders are built with higher and higher energies. By pushing the energy frontier further, physicists hope to discover new particles and phenomena that have never been observed before.

1.3.1 Why a Muon Collider?

One of the main obstacles in the use of electron positron colliders is the presence of synchrotron radiation. Every charged particle running in a circular trajectory emits electromagnetic radiation proportional to the inverse of its square mass. Because proton mass is about 1 GeV and the electron one is about 0.5 MeV comparing the radiation emitted by the two, a lot more is lost in a lepton collider. This is the reason proton-proton colliders have been built, with such a machine it is easier to reach higher energies. The use of protons leads to a complication, according to QCD they are composite particles made of partons, quarks, which presence inside it is described statistically through parton distribution functions. The partons, in a proton collision, only just takes a part of the energy of the entire proton, so not all the machine energy is carried by it. Because of the nature of the proton, also a huge QCD background happens in the collision, an aspect not present in a lepton collider where the background is way more clean.

This being sad, it is clear that a hadron collider is better for the energy frontier, and the electron positron machines are good for precision measurements. Here the possibility of a muon colliders come in to play; muons are heavier than electrons ($m_\mu = 105.7$ MeV), they will have fewer problems of syncrotron radiation; also, being pointlike they would have all energy available in the center of mass to perform the collision and the background would be cleaner w.r.t. the one in a collision of composite particles. A muon collider would, in this way, combine both advantages of precision and energy, now separately present in the two collider options today available.
To overcome the problem of synchrotron radiation the efforts could be pointed toward a linear electron-positron accelerator; there are some concepts of future linear machines working with electron positron beams, like the CLIC (Compact Linear Collider) or the ILC (International Linear Collider), but to reach high energies an extremely long apparatus is required.

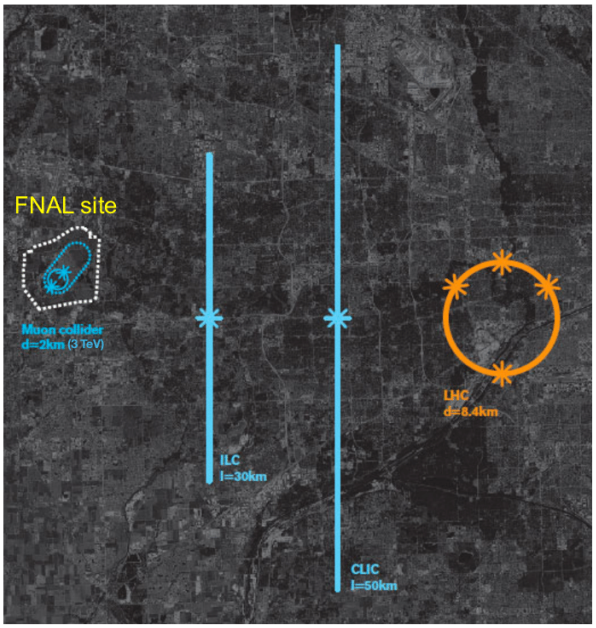

Figure 1.5: Size of a future muon collider (on the left) compared to the ones of ILC, CLIC (two straight lines) and LHC (orange circle)

We can compare in Fig.(1.5) the dimension of a possible future muon collider and the ones of two concepts of linear machines and the existent LHC.
In building a muon collider, the main difficulty is not in how to reach high energies, but in how to produce high luminosity beams, meaning one with controllable energy, intensity and with low angular and energy spread. Muons can be produced mainly in two ways, through pions decay or in electron positron collision. By producing them with pions decay, it is possible to obtain a high luminosity but, when produced in this manner, they are not collimated in a compact beam; this problem leads to the challenging practice of cooling, necessary to create a beam with low spread in position and momentum space(6D cooling). If the muons are produced in a collision of electron positron with one of the initial particles at rest, we would have a boosted and collimated production of muons but, in this case, the problem would be to reach a high luminosity.
There is also another challenge: muons are not stable particles, they have a very short lifetime, $2\,\mu$s; because of this, while it is needed to push to high momentum the beams to extend the laboratory frame lifetime up to orders of seconds, the exponential decay of

the muon would produce an intense shower of electrons, resulting in a background noise for the apparatus and the physics measurements would be strongly affected by this. In addition, the products of decay in the interaction with the machine-detector components could affect its performance. For this reason, mitigation strategies have to be applied in order to perform measurements. If difficulties in producing muons are not overcome, a muon collider would remain a dream, but the technological challenges that arise do not appear to be insurmountable, on the contrary are a big opportunity to develop new experimental techniques. In case of success there is one case in which, even at low energies, the built of a muon collider would be of big interest and exceeding the possibilities of lepton colliders working at the same energies. Would be the case of a muon collider working at 125 GeV. At this energy we would have a Higgs Factory with an efficiency of order 10^4 bigger w.r.t. one based on electron positron collision. If going at high energies will result not just a fantasy, a muon collider at 30 TeV would be a dream machine, combining energy and precision together.

It is interesting to compare a muon collider with a hadron collider performances; in doing this one could consider the c.m. energies at which the two apparatus have the same cross section. As already mentioned, for protons, the center of mass energy of the collision is divided among the partons that constitute it and the partonic energy available for the collision is distributed statistically between them. For this reason, a muon collider generates interaction across all values of $\sqrt{s}$ while the latter is dominated by regions where $\sqrt{\hat{s}} \ll \sqrt{s}$ where $\sqrt{\hat{s}}$ correspond to the partonic c.m. energy and $\sqrt{s}$ to the c.m. energy for the entire proton. It is important to notice that when comparing a collision of two particles in the production of new ones in two different colliders has to be taken in account the different physics happening in this production. If we are interested in the production of a state in the two different colliders this production will result, for example, of QCD nature in a proton collider and of electroweak nature in a muon one; this results in an enhancement of one of the two in respect to the other and to compare the total cross sections one need to take into account for differences between QCD and electroweak partonic cross sections

$$\beta = \frac{[\hat{\sigma}]_p}{[\hat{\sigma}]_\mu}, \tag{1.11}$$

In [3] and [4] is reported that for a 2 particle collision process producing a massive particle X plus other products, assuming comparable partonic cross sections for the production of such particle X, the value of cross section reached in a pp collider at 100 TeV can be matched with $\sqrt{s_\mu} \simeq 20$ TeV at a muon one. The previous advantage, can be even higher in a process where a pair of heavy states is produced, as to reach the same cross section value is needed $\sqrt{s_\mu} \simeq$ 5-7 TeV. Even with β=10 this last process would be resembled in a muon collider with $\sqrt{s_\mu} \simeq 12$ TeV. We understand that a muon collider, given an energy and luminosity, is way more effective than a proton collider with comparable energy and luminosity.

Chapter 2

Electroweak Sudakov logarithms and their implementation

In this section, after the introduction where we have revisited the fundamental concepts of cross section, perturbative expansion and the main novelties that a muon collider would bring, let focus on what the so called Sudakov terms are, where they appear in the perturbative expansion and the story of their implementation.
For a given process when we go to NLO calculations, meaning we consider in the cross section terms of higher order in the expansion parameter, begin to appear terms that describe interference between different amplitudes, tree-level ones and the ones that comes in to play just at NLO. What happens in amplitude calculations is that the LO one, $\mathcal{M}_0$, that encodes the information about the tree-part level of the process, receives corrections from the amplitude $\mathcal{M}_1$, which contains the one-loop contributions. So the amplitude, at one-loop accuracy, will be

$$\mathcal{M} = \mathcal{M}_0 + \mathcal{M}_1, \tag{2.1}$$

where unlike Eq(1.7) we have understood the dependence on α. This is the starting point to build the cross section at NLO, and including amplitudes at even higher order is the way to go to NNLO or even higher.
Now we see in what the Sudakov approximation consists and to better understand it let consider a general EW process at scale s; if we look at the one-loop EW virtual corrections of $\mathcal{O}(\alpha)$, in general they have this form:

$$\mathcal{M}_1 = \mathcal{M}_0 \frac{\alpha}{2\pi}\Big[\text{constant}+\mathcal{O}(\frac{M_W^2}{s}) + \mathcal{O}(\log^k(\frac{s}{M_W^2}))\Big], \tag{2.2}$$

with $k = 1, 2$ in according to Eq.(1.10), and M_W the mass of the W boson.
The singular and double logarithmic terms when we perform calculations at high energies, meaning big $\sqrt{s}$, become the dominant ones in the expansion. Indeed, it is sufficient to consider that for a value of M_W around 80 GeV and $\sqrt{s}$ of 1 TeV the comparison between the last two terms in equation (2.2) is in favor of the logarithmic terms, allowing us to keep only these and still have a good enough approximation of the full (2.2).
This is the reason the Sudakov proposal, in approximating the full (2.2) with just the log term, is a good approximation just for large scale s processes. Basically, these logarithmic terms are the one the literature refers to as Sudakov ones.

2.0.1 The DP Algorithm

The work [1] is the first that proposed at pure amplitude level the calculation of both single-logarithms (SL) and double-logarithms (DL) one-loop virtual EW Sudakov corrections for a general process. That work focused on the logarithmic behavior of the one-loop matrix element, and pioneered the way to have a reliable approximation of the latter, much simpler and faster to compute. Indeed, at the time when [1] appeared, NLO computations which are by now fully automated [2], still required a substantial effort, particularly those where involving multiple mass-scales, such as the calculations of electroweak corrections.

Recently, despite the aforementioned automation of EW corrections, various Monte-Carlo groups have shown interest in the algorithm of [1], since it makes it possible to obtain more efficiently the dominant contribution to EW corrections. Furthermore, some changes w.r.t the original algorithm have been proposed, in particular in [2] where the algorithm has been implemented in the MadGraph5_aMC@NLO framework. These changes aimed at improving the approximation of [1] on several aspects which are crucial to have the algorithm implemented in modern Monte-Carlo codes, and to obtain reliable predictions for physical quantities.
In this chapter, we will briefly review this journey, starting from the work in [1] and looking at the improvements proposed in [2].
The starting point of the work[1] is in writing the general form of the logarithmic contributions to the logarithmic approximation, namely the followings terms:

$$L(|r_{kl}|, M^2) := \frac{\alpha}{4\pi} \log^2(\frac{|r_{kl}|}{M^2}) \quad \text{and} \quad l(|r_{kl}|, M^2) := \frac{\alpha}{4\pi} \log(\frac{|r_{kl}|}{M^2}), \tag{2.3}$$

that depend on different invariants r_{kl} and masses M related to the Feynman diagrams they originate from, and

- The DL contributions originate from one-loop diagrams where soft-collinear gauge bosons are exchanged between a pair of external legs and represent a leading and negative correction
- The SL contributions from loop diagrams originate from the emission of virtual collinear gauge bosons from external lines and often have opposite sign and are referred to as the subleading ones.

In [1] amplitudes of processes were considered with all external particles on shell in the limit where all invariants are much larger than the gauge-boson masses,

$$r_{kl} = (p_k + p_l)^2 \approx 2p_k p_l \gg M_W^2 \simeq M_H^2, M_W^2, M_Z^2, m_t^2, \tag{2.4}$$

with k and l indices to indicate two generic external particles and p_k,p_l their momenta. In general the invariants are the standard Mandelstam ones s, t, u but in a scattering process with more than four total external particles there are more, this is the reason we call them r_{kl}.
The approximation of massless particles is a valid one because as we said previously this logarithmic approximation just works for processes at high energies. If we are not in the regime of Eq.(2.4) the second term in the equation (2.2) would not be negligible and taking just the logarithmic part would not be a good approximation to the one-loop virtual

NLO EW amplitude because of the presence of the other terms. If the logarithmic term is not large the Sudakov approximation is not a good approximation, this is the reason of the condition (2.4).
This kind of approximation, that retains the enhanced DL and SL of the form of Eq.(2.3) is called logarithmic approximation LA.

In order to render the results as symmetric as possible, all logarithmic terms have been parameterized by the following ones

$$L(s) := L(s, M_W^2) \quad \text{and} \quad l(s) := l(s, M_W^2), \tag{2.5}$$

in order to relate the energy-dependent part of all large logarithms to the scales s and M_W. To do so one just need to rewrite the logarithmic part of the first element of (2.3) as such

$$L(|r_{kl}|, M^2) = \log^2(\frac{|r_{kl}|}{M^2}) = \Big[\log(\frac{r_{kl}}{s}) + \log(\frac{s}{M^2})\Big]^2 \tag{2.6}$$

$$= L(s, M^2) + 2l(s, M^2)\log\frac{|r_{kl}|}{s} + L(|r_{kl}|, s) = \tag{2.7}$$

and finally

$$= L(s) + 2l(s)\log\frac{M_W^2}{M^2} + L(M_W^2, M^2) + L(|r_{kl}, s|) + 2l(s)\log\frac{|r_{kl}|}{s} + 2\log\frac{M_W^2}{M^2}\log\frac{|r_{kl}|}{s}. \tag{2.8}$$

In this work the authors relied on the assumption that all invariant are comparable one to the other

$$r_{kl} \simeq r_{k'l'} \tag{2.9}$$

and that just allows us to take the non negligible part of Eq.(2.8), the following

$$L(|r_{kl}|, M^2) := L(s) + 2l(s)\log\frac{M_W^2}{M^2} + 2l(s)\log\frac{|r_{kl}|}{s}, \tag{2.10}$$

neglecting logarithmic terms that look like these:

$$l(M_W^2, M_Z^2), \qquad l(m_t^2, M_W^2), \qquad l(M_H^2, M_W^2), \qquad \log(|r_{kl}|/s), \qquad \log^2(|r_{kl}|/s). \tag{2.11}$$

These are the assumptions under which, in the pioneering work [1], the calculation of the Sudakov logarithms for a one-loop EW amplitude was possible.
In Eq(2.10) can be individuated two kind of terms, we identify the first two as leading soft collinear(LSC) and the last as subleading soft collinear(SSC).
After the individuation of all the non negligible logarithmic terms they wrote the Sudakov approximation of the virtual one-loop amplitude; introducing the following notation

$$\mathcal{M} = \mathcal{M}_0 + \mathcal{M}_1 = \mathcal{M}_0 + \delta\mathcal{M} = \mathcal{M}_0 + \mathcal{M}_0\delta. \tag{2.12}$$

We can write the Sudakov approximation term as in [1] with all its contributions:

$$\delta = \frac{\delta\mathcal{M}}{\mathcal{M}_0} = \delta^{LSC} + \delta^{SSC} + \delta^{C} + \delta^{PR}. \tag{2.13}$$

The terms δ^{LSC} and δ^{SSC} comes from the diagrams where gauge-bosons are exchanged between external legs and are soft collinear, δ^{C} comes from logarithms originating from

virtual collinear gauge-bosons from external lines and from field renormalization constants.The last comes from the parameter renormalization, like, for example, QED coupling or weak mixing angle.

Now that we have done a brief overview of the work by Denner and Pozzorini it is time to focus on some aspects of their derivation. Let's start highlighting an aspect of enormous importance in perturbative calculations. In NLO EW corrections, when photons are involved, we have to face the problem of IR divergences; infinite large terms in our amplitudes are not something in tune with physical predictions. From the very beginning of these calculations in the context of Sudakov approximation of one-loop virtual amplitudes has been known that this kind of divergent terms are cancelled by their real counterpart in the inclusive calculations of cross sections, giving a reliable prediction.
The standard approach for employing the Sudakov approximation consisted of simply dropping the divergent terms and keeping the finite one. This has been the reason of some necessary revision of the method used in [1] as we will see in the following.

2.0.2 Revisitation of the DP Algorithm

Now we review the work [2] where has been performed a revisitation of [1], giving a new prescription for the NLO EW calculations. In [2], some extension of the original work of Denner&Pozzorini were carried out, those relevant to the work of this thesis are

- The masses of photons and light-fermions are set exactly to zero and the regularization of IR divergences is performed by Dimensional Regularization techniques.
- Exclusion of divergent QED component (photons) to keep only the weak one (W and Z bosons) leads to a better approximation of NLO EW corrections.
- Taking into account additional angular dependencies without assuming that all invariants are of the same size of the center of mass energy $\sqrt{s}$, meaning violation of Eq.(2.9)
- Identification of an imaginary term that was omitted in [1] that cannot be generally neglected for a $2 \to n$ process with $n > 2$.

In [1] IR singularities are regularized by an infinitesimal photon mass λ that has been inserted so that in calculations one could produce finite answers and, after individuating the terms responsible for the divergence, just drop them. Here we will show an example of the removal of an IR divergent term with the [1] approach.
Consider the δ^{LSC} term of Eq.(2.13), its form, calculated in [1], is the following:

$$\delta^{LSC}_{i'_k i_k}(k) = -\frac{1}{2}\Big[C^{ew}_{i'_k i_k}(k)L(s) - 2(I^Z(k))^2_{i'_k i_k}\log\frac{M_Z^2}{M_W^2}l(s) + \delta_{i'_k i_k}Q_k^2 L^{em}(s,\lambda^2,m_k^2)\Big], \quad (2.14)$$

with the last term being

$$L^{em}(s,\lambda^2,m_k^2) \equiv 2l(s)\log(\frac{M_W^2}{\lambda^2}) + L(M_W^2,\lambda^2) - L(m_k^2,\lambda^2), \quad (2.15)$$

with $i'_k i_k$ the indices of the two external legs the terms are referred to, k one of the external particles, C^{ew} the Casimir operator and $(I^Z(k))^2$ the squared Z-boson coupling

the expressions of which can be found in Appendix A of [1].
The term L^{em} contains part of the terms of electromagnetic origin, and in particular the divergent ones.
In order to cancel the IR divergences, present in this term, the first approach was to remove it, ensuring the possibility to obtain finite results.
This choice, producing finite results, allowed to use later Denner and Pozzorini's work for the implementation of an automated algorithm in MadGraph that could calculate the Sudakov approximation in NLO EW calculations, a prescription that, as in literature, we will refer to as SDK0 in Chapter 3.
What is the problem in such approach?
Removing all terms tagged as "em" really just isolates the photon contribution from the scale λ^2 to M_W^2 leaving the part present at the scale that span from M_W^2 to the scale s of the process. While in the case of purely weak contributions the dependence on M_W^2 is physical, in the case of QED the separator of the two scales M_W^2 here has just the function of technical separator of logarithms, but could have been any other value between λ^2 and $\sqrt{s}$; it only depends on the convention used in the original formulation of Denner and Pozzorini.
These considerations brought to the need of removing divergences following another approach based on selecting only the DL and SL of purely weak origin, excluding the contributions of QED origin from amplitudes. Indeed, for sufficiently inclusive observable, most of the logarithms of QED origin cancel against their real-emission counterpart, so keeping only the pure weak one will lead to a better NLO EW approximation.
The implementation of the algorithm where divergences are removed in this way, removing completely the QED contribution, we will refer to as SDK_{weak} and we will confront the result obtained with it with the one given by the different prescription SDK0, where the approach was just to drop the "em" tagged terms.
As said in the previous section, all invariants have been considered much larger than gauge-bosons masses, see Eq.(2.4) and all Sudakov terms have the form of Eq.(2.3). The modifications introduced in [2] take care of the violation of the condition

$$r_{kl} \simeq r_{k'l'} \tag{2.16}$$

In this new regime we now can include new logarithmic terms that have been previously discarded, of the form

$$\frac{\alpha}{4\pi}\log^2\left(\frac{r_{kl}}{r'_{k'l}}\right) \quad \text{and} \quad \frac{\alpha}{4\pi}\log\left(\frac{r_{kl}}{r_{k'l'}}\right), \tag{2.17}$$

in a way that improves the quality of the Sudakov approximation of EW corrections, as we will show in Chapter 2. The choice of considering valid or not the condition (2.16) cannot be made a priori because the result of the approximation of NLO EW is a process dependent matter, so it is always a good habit to confront the result obtained with and without this new angular term with the NLO EW value.

The last improvement we will give a glance to, consists in the identification of an imaginary term that was previously discarded that results, in addition with the departing from condition (2.16), in an overall change of Eq.(2.10) in to this one

$$L(|r_{kl}|, M^2) - 2i\pi\Theta(r_{kl})l(|r_{kl}|, M^2) = \tag{2.18}$$

$$= \underbrace{L(s) + 2l(s)\log\frac{M_W^2}{M^2}}_{\text{LSC}} + \underbrace{2l(s)(\log\frac{|r_{kl}|}{s} - i\pi\Theta(r_{kl}))}_{\text{SSC}} +$$

$$\underbrace{2l(M_W^2, M^2)\log\frac{|r_{kl}|}{s} + L(|r_{kl}|, s) - 2i\pi\Theta(r_{kl})l(|r_{kl}|, s)}_{\text{SSCstorkl}} + ...$$

The elements of the third line become relevant only when $s \gg r_{kl} \gg M$ so when we are not respecting (2.16).
In the next Chapter we will use both approaches SDK0 and SDK$_{weak}$ with the inclusion or not of the angular terms coming from violation of Eq.(2.16) to confront and eventually see the benefits of the work [2]. It is important to notice that in the version of MadGraph used here, the code has implemented the presence of the imaginary term we talked about, so actually the SDK0 approach used for our results is not really the standard SDK0 coming from [1].

Chapter 3

Numerical results

3.1 Setup of MadGraph

In this section, we look at the basic setup of MadGraph, in order to resemble a realistic collision experiment and to optimizing the Monte Carlo integration. We used the same parameters of [2]; all SM particles, except the followings, are considered massless, and all decay widths are set equal to zero except for the ones of Z and W bosons.

$$m_Z = 91.118 \text{ GeV}, \quad m_W = 80.385 \text{ GeV}, \quad m_H = 125 \text{ GeV},$$

$$m_t = 173.3 \text{ GeV}, \quad \alpha_s(M_Z) = 0.119, \quad G_\mu = 1.16639 \cdot 10^{-5} \text{ GeV}^{-2}.$$

Moreover, we adopted, in the case of hadron collider, from the set NNPDF3.1, the distribution NNPDF31_nlo_as_0118_luxqed.
We started the investigation with some processes in hadron collider, in this case, when the two protons collide, the probability to find a parton inside a proton with momenta equal to the fraction x of the total proton momenta changes w.r.t. the scale we look to the process, the so-called factorization scale; this probability is described by the so-called Parton Distribution Functions (PDFs) that are regulated by the factorization scale (μ_F) that we set equal to the partonic center of mass energy $\sqrt{\hat{s}}$, so as for the renormalization scale (μ_R) of α_s.

3.1.1 Cuts and clustering

Phase space cuts are a way of reducing the events that are generated in a simulation. In order to match a desired accuracy, for example, if one is interested in studying a specific process that only produces events with a certain minimum energy or transverse momentum, the desired constraints on these quantities can be imposed to exclude events that do not satisfy them.
In our specific work, to resemble realistic experimental cuts for high-energy objects and avoid additional logarithmic enhancements from collinear splitting, we impose cuts on quantities like invariant masses, pseudorapidities, transverse momenta and the distance in pseudorapidity and azimuthal angles between particles.
This is possible with MadGraph thanks to its user-friendly structure, which allows us to set standard cuts, or for more specific requests, implement custom cuts in the Fortran code.

What is the difference between the two? A standard cut resizes the phase space to the region of our interest and then leaves the Monte Carlo simulation to generate events in this region; in doing so, given a simulation that generates a certain amount of events, we do not lose any of them, neither efficiency, due to the excluded region; when a custom cut is imposed, the simulation generates a certain amount of events in the full phase space region, and only after this, the region we are not interested in is removed, resulting in a general loss of efficiency.
So the first option is the safest and the one that requires less human intervention, and allows for different types of cuts to be applied at different stages of the event generation process, such as at the parton level or at the hadron level.
With the second opportunity it is possible that one could exclude too many events that would be generated, giving to MadGraph a very little number of events to deal with, resulting in an insufficient statistic and impossibility to carry on the simulation.

Because we look for differential distributions of IR-safe observables, bare leptons l have to be recombined with photons γ in dressed leptons.
This corresponds to the following condition,

$$\Delta R(l,\gamma) = \sqrt{(\Delta\eta(l,\gamma))^2 + (\Delta\phi(l,\gamma))^2} < 0.4, \tag{3.2}$$

where $\Delta\eta(l,\gamma)$ and $\Delta\phi(l,\gamma)$ are the differences of the bare-lepton and photon pseudo-rapidities and azimuthal angles. Also, photon recombination cancels the virtual QED contributions associated to the collinear configuration of the final state, which is precisely what is taken into account by the approach followed in the revisitation [2]. In addition, we performed the recombination of photons also with any other electrically charged particle, including top quarks and W bosons. These settings will be adopted in the simulations displayed in the following chapter.

3.2 Hadron Collider

In this chapter, in order to acquire some familiarity with MadGraph we reproduced some results obtained in Section 6 of [2], two processes at Hadron Collider at 100 TeV which is one of the possible experimental set-ups that has been considered as an option for a high-energy future collider. The processes that we considered are two: separately electron-positron and three Z bosons production, both from proton proton collision:

$$pp \to e^+e^-,$$

$$pp \to ZZZ,$$

and at these energies LA is expected to capture NLO EW effects in a very efficient way. For the processes that we are going to analyze we do not need to consider renormalization scale in MadGraph, because even if the coupling constant α runs, in the code is renormalized in on-shell scheme, so the scale is fixed.

The analysis we performed classifies the particles in the final state with respect to their hardness, meaning the value of their transverse momentum. In a process like the

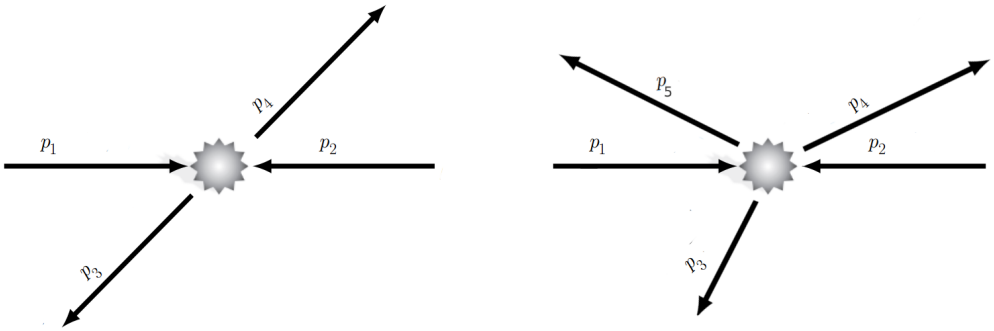

Figure 3.1: Left: kinematic in the c.m. of a $2 \to 2$ collision of two identical particles of 4-momenta p_1,p_2 producing a pair of identical particles of 4-momenta p_3,p_4. The produced particles are back-to-back due to momentum conservation, so they have the same value of transverse momentum, dependent on the collision conditions. Right: in a collision of the same two particles with production of three particles of momenta p_3,p_4,p_5 the products, because of momentum conservation, will result going on three different directions.

one that produces two equal leptons, at LO, we have back to back particles so that they are equally hard as shown in Fig3.1, but this is not true at NLO where the recoil of a particle with a photon could create a hierarchy in their hardness.

The results are presented to compare the exact NLO EW value to their LA, obtained according to the two prescriptions SDK0 and SDK$_{weak}$ presented before; as we said the term $SSC^{s\to r_{kl}}$ of Eq.(2.18) can be either included or not, the first case refers to the solid lines, the second to the dashed ones in the plots.

3.2.1 $pp \to e^+e^-$

We begin with the production of e^+e^-, imposing the following cuts:

$$p_T(e^\pm) > 200 \text{ GeV}, \quad |\eta(e^\pm)| < 2.5, \quad m(e^+, e^-) > 400 \text{ GeV}, \quad \Delta R(e^+, e^-) > 0.5, \quad (3.3)$$

where the quantities are: p_T, the transverse momentum, η, the pseudorapidity, m the dilepton invariant mass and ΔR is explained in Eq.(3.2).

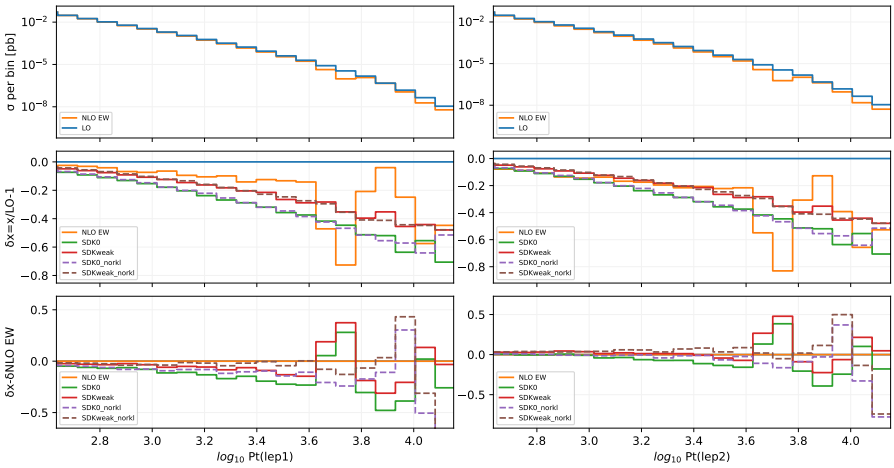

Figure 3.2: Differential cross section for recombined leptons in $pp \to e^+e^-$ at 100 TeV at LO and at NLO EW. Comparison between NLO EW predictions and its LA in different approaches, namely SDK0(green), SDK$_{weak}$(red) with(solid) and without (dashed) SSC$^{s\to r_{kl}}$term

We will use the same layout we use for Fig. 3.2 for all plots in the next chapters: in the top charts, we show the differential distribution at LO and at NLO EW accuracy. For a certain value of transverse momentum, denoted by a vertical red line, it could happen that the NLO EW predictions, meaning LO + NLO EW corrections, turn to be negative, so we plot its absolute value. In the medium charts, we show the relative impact of EW correction in the various approximations, $\delta_X \equiv X/LO - 1$. The solid orange line represents the exact $\mathcal{O}(\alpha)$ correction, and the other lines are the calculations performed with different procedures. The green SDK0 line is the one resulting from the prescription described in Chapter 1, meaning the standard Sudakov calculation, the red lines are the result of the "SDK$_{weak}$" approach. The closer a line is to the NLO EW, the better the line approximates it. In order to appreciate it, we inserted at the bottom of the Fig. 3.2 the charts built subtracting $\delta_{NLO\,EW}$ from the relative difference δ_X.

In Fig.3.2 we see that the transverse momentum ranges from $\sim$ 400 GeV to $\sim$ 14000 GeV and the NLO EW corrections reach $\sim$ -70% of the LO in the tail; in the second plot we see that as p_T grows, fluctuations of the curves start to be very significant, especially the ones that affect the NLO EW curve.
The reason for the larger oscillations of the NLO EW curve is that, in the calculations of it, Born, real and virtual contributions are defined in two different phase spaces, the real contribution phase space has one more particle than the one of the virtual and Born.

When the exact NLO EW prediction is calculated, challenges arise both because the evaluation of virtual diagrams is very CPU demanding, and because of large cancellations with contributions from real radiation. Indeed, schematically defining NLO=V$\oplus$R where V is the virtual and R is the real, if $|V|$,$|R| \gg |NLO|$ a given precision on NLO requires a much higher precision for V and R. Instead, Sudakov approximations are calculated in the Born phase space only, as one can see from Eq.(2.12), and their form is analytic; the cancellation is already taken into account in the SDK$_{weak}$ approach and partially in the SDK0. This is the reason why in the Sudakov predictions, fluctuations are much smaller. Because of this behavior, present from the tail region and forward, we decide to plot the quantities up to a point that still allows us to appreciate their trend. In the same plot we see that the red solid line representing the SDK$_{weak}$, up to regions where big fluctuations interrupt the smooth behavior, has a smaller distance from the NLO EW orange correction, meaning this one is better approximated by this method than SDK0. This is better represented in the last inset of Fig.3.2 where, as before, the red line (SDK$_{weak}$) is closer to the one of the NLO EW.

3.2.2 $pp \to ZZZ$

The next process at Hadron Collider is triple Z production, on which we applied the following cuts:

$$p_T(Z_i) > 1000 \text{ GeV}, \quad |\eta(Z_i)| < 2.5, \quad m(Z_i, Z_j) > 1000 \text{ GeV}, \quad \Delta R(Z_i, Z_j) > 0.5, \tag{3.4}$$

where the quantities are referred to every possible pair of the products, with $i, j = 1, 2, 3$.

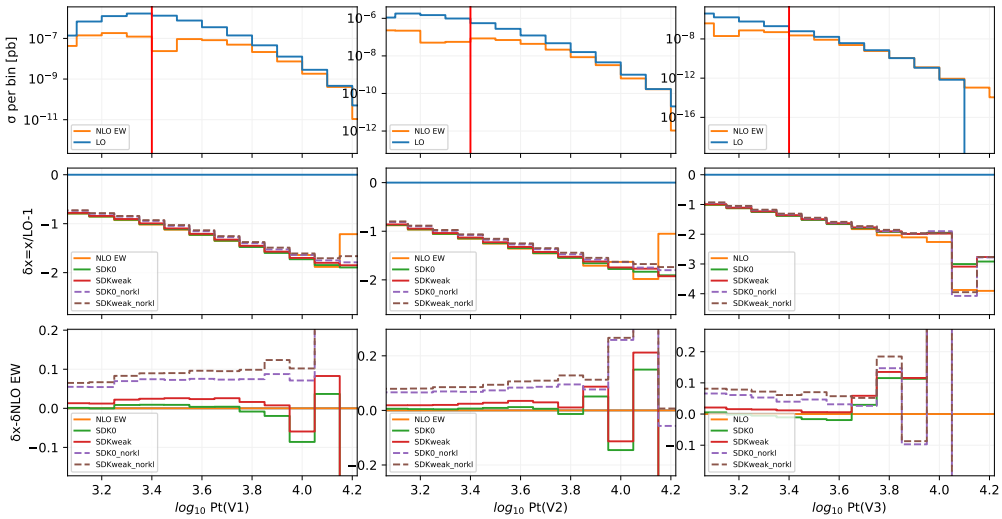

Figure 3.3: Same as Fig. 3.2, but for ZZZ hadroproduction at 100 TeV

In Fig. 3.3 we plotted the differential distributions for the three products of the reaction, ordering them from the hardest to the softest, from the left to the right. Here the NLO EW predictions are already, for low values of p_T, negative, as we can see in the medium charts, reaching, in absolute value in the last part of the tail, a magnitude of 100% the LO value, meaning that the NLO EW corrections can reach up to -200% of LO.
The negative value of the LA means that we have a non-physical result at this order in the expansion; in order to retrieve a sensible result, resummation of the EW corrections, in particular of their high-energy component, is necessary. However, we will not consider this aspect in this work.
For this process, the difference between the approach with and without the angular term $SSC^{s \to r_{kl}}$ is more evident than the previous process. In the previous production of leptons the SDK0 and SDK$_{weak}$ lines are near to their counterpart without the angular factor, here we see a constant and visible separation between the solid and dashed lines. We can expect this, because in a $2 \to 3$ we have a richer hierarchy of invariants w.r.t. a simple $2 \to 2$ process.
We see in the third inset of Fig. 3.3, representing the quantity $\delta_X - \delta_{NLO\,EW}$, that the SDK0 and the SDK$_{weak}$ with the factor $SSC^{s \to r_{kl}}$ are contained in a region where the plotted quantity is under the value of 5%, instead the two without the factor reach the value of 10%; also here fluctuations start to appear as p_T grows making the analysis no more reliable at a certain point.
Now we start to simulate the same two processes and others at Muon Collider.

3.3 Muon Collider

In this section we consider the four following processes using MadGraph, simulating a Muon Collider at the energies of 3,10 and 30 TeV.

$$\mu^+\mu^- \to e^+e^-, \quad \mu^+\mu^- \to W^+W^-, \quad \mu^+\mu^- \to t\bar{t}, \quad \mu^+\mu^- \to ZZZ.$$

3.3.1 Differential distributions

In this section, in each figure we collect plots for the three different energy regimes for the same process, and each plot will have the same layout as the ones of the previous section. This, in addition with the new dynamic happening at Muon Collider, will allow us to grasp informations about the genuinity of the various approaches in the calculation of the NLO EW approximation, and to appreciate the modifications made to the old algorithm thanks to the revisitation of [2].
As recalled in the early chapters, a Muon Collider is way more efficient than Hadron Collider at the same energy, and also a new dynamic of the collision is present; these factors will be manifest in the plots, where a new behavior of the differential cross section arise giving the possibility to make sense of the different approaches used to approximate the NLO EW cross sections.
Because of the different scenario we are in, we also need to change some parameters in MadGraph to resemble the new kind of collider. The energy available to the collision now is the full $\sqrt{s}$ value, so we use fixed renormalization and factorization scales, setting $\mu_R = \mu_F = \sqrt{s}$.
We also impose some cuts on the phase space of final particles for resembling realistic experimental cuts: on the first three processes we impose the followings:

$$p_T(P) > 200 \text{ GeV}, \quad |\eta(P)| < 2.5, \quad m(P_i, P_j) > 400 \text{ GeV}, \quad \Delta R(P_i, P_j) > 0.5, \tag{3.5}$$

with P the particles produced in the first three processes.
The cuts for the last process are these:

$$p_T(Z) > 500 \text{ GeV}, \quad |\eta(Z)| < 2.5, \quad m(Z_i, Z_j) > 500 \text{ GeV}, \quad \Delta R(Z_i, Z_j) > 0.5, \tag{3.6}$$

where these quantities are referred to every possible pair of Z bosons, with $i, j = 1, 2, 3$.
Because of the different dynamic of this process, we will report also the differential distributions w.r.t. the values of invariant mass of all possible pairs of Z bosons produced.
For the $2 \to 2$ processes, the study of the differential distribution w.r.t. the invariant mass gives us the same information that can be derived from the study of the total cross section values.
We begin studying the process $\mu^+\mu^- \to e^+e^-$ that in the context of QED is one of the most interesting, indeed the reversed one is used in high-energy physics to calibrate the machines that are used to study e^+e^- collisions. In our work we are interested at it in the more complete landscape of SM where also gauge bosons come in to play.
We will witness from the beginning, because of the different dynamic happening at a Muon Collider, a different behavior of the differential distributions.

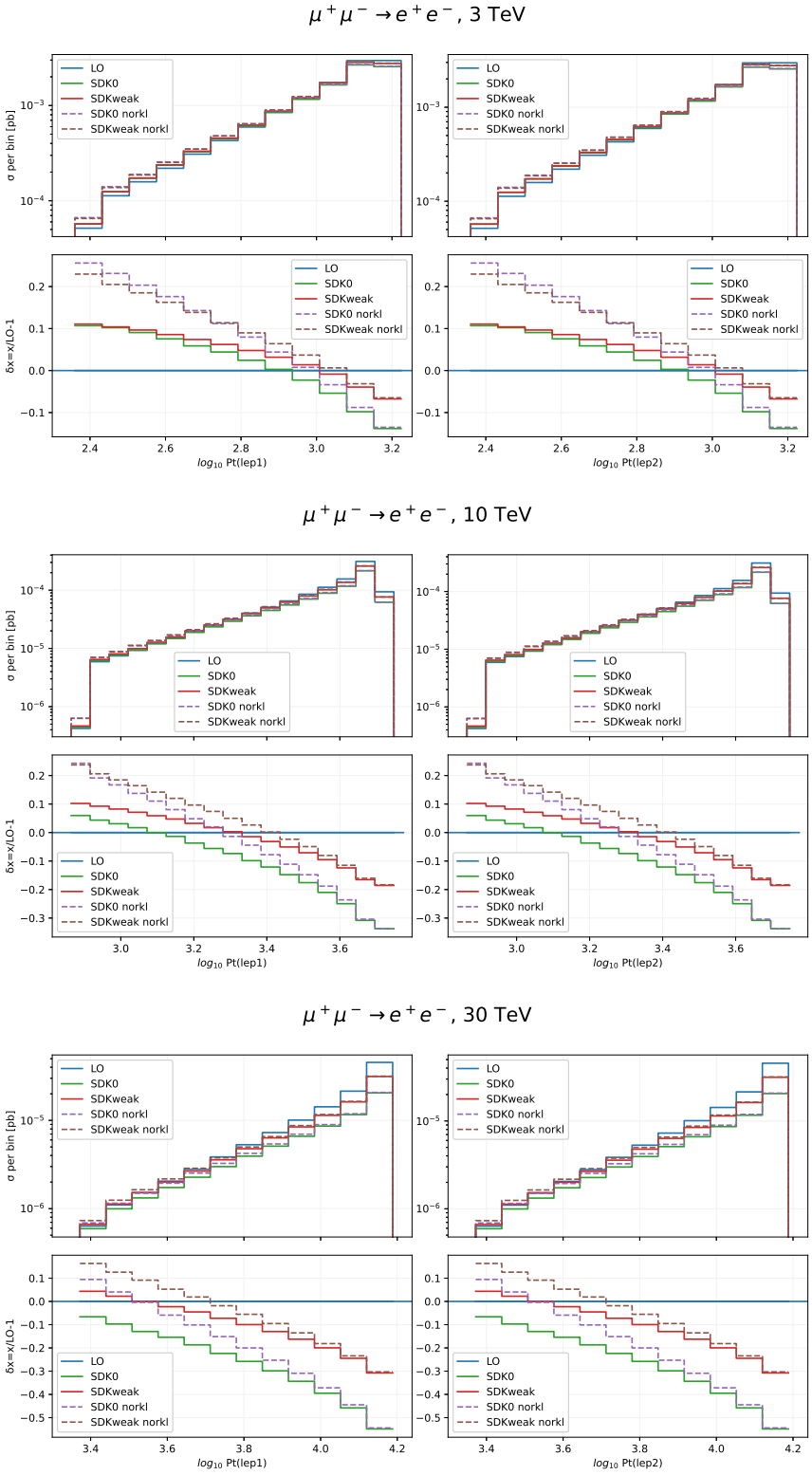

Figure 3.4: Differential cross section for recombined leptons in $\mu^+\mu^- \to e^+e^-$ at 3,10 and 30 TeV at LO and at LA with different approaches, namely SDK0, SDK_{weak} with (solid) and without (dashed) $SSC^{s\to r_{kl}}$term. In the bottom inset of each energy group is shown the relative magnitude of each LA w.r.t. the LO.

We see in Fig. 3.4 that the p_T distribution, for every energy, grows with the transverse momentum, in opposition with the one of the same process in the other collider. The biggest contribution to the cross section at LO is at high p_T because at LO the diagram of the process consists of only an s-channel. Indeed, we do not have an enhancement given by a possible t-channel, leading to larger contributions, at low p_T.
For example, if we considered the process

$$\mu + \mu - \rightarrow \mu + \mu -$$

then there would have been both s-channel and a t-channel that would have made the two outgoing particles to be collinear to the ones in the initial state to increase the cross section.

The bottom plots of every group of Fig.3.4 show the relative impact of the EW corrections in different approximations, $\delta_X \equiv X/LO - 1$. We see that at 3 TeV and in the low p_T region, the difference between the two approaches SDK0 and SDK$_{weak}$, where they bring a positive correction to the LO, is tiny, they both reach $\sim$ 11% of the LO value; in this same region is very relevant the presence of the angular factor $SSC^{s \rightarrow r_{kl}}$ in the approaches, they both reach $\sim$ 23-25% of LO value. At high p_T SDK0 reaches $\sim$ -14% of LO and SDK$_{weak}$ $\sim$ -7%; they are completely different one to the other but near to their counterpart with $SSC^{s \rightarrow r_{kl}}$ factor on.
The $SSC^{s \rightarrow r_{kl}}$ factors take care of situations where there is a hierarchy between invariants. For large p_T like 1500 TeV both t and s are large and comparable. I have big invariant t and big invariant s, so they are comparable. At low p_T we have small t and big s so the calculations of Sudakov terms with $SSC^{s \rightarrow r_{kl}}$ factor on is really different to the calculations without this factor.
At 30 TeV the situation is very similar, in the low p_T region the approaches without the $SSC^{s \rightarrow r_{kl}}$ factor are distant to their counterpart with it, but much more that at lower energies; their lines are separated in the whole region from low p_T to high p_T, where they meet their counterpart. Going to higher energies the relative impact of the various Sudakov corrections become larger, in this energy regime we reach, in the high p_T region, an impact of $\sim -55\%$ of LO with SDK0 and of $\sim -30\%$ of LO with SDK$_{weak}$.
We see that as more the energy grows, the more the contribution of Sudakov logarithms become negative w.r.t. LO.

The cause of the general discrepancy between the SDK0 and SDK$_{weak}$ approaches is because they are a different treatment of QED logarithms that come from photon emission from leptons, and these logarithms depend on invariants r_{kl} and therefore also on the p_T of the lepton. Since we consider dressed leptons, our differential observables are inclusive on photon emissions of any hardness. This renders the SDK$_{weak}$ approach more reliable than the SDK0

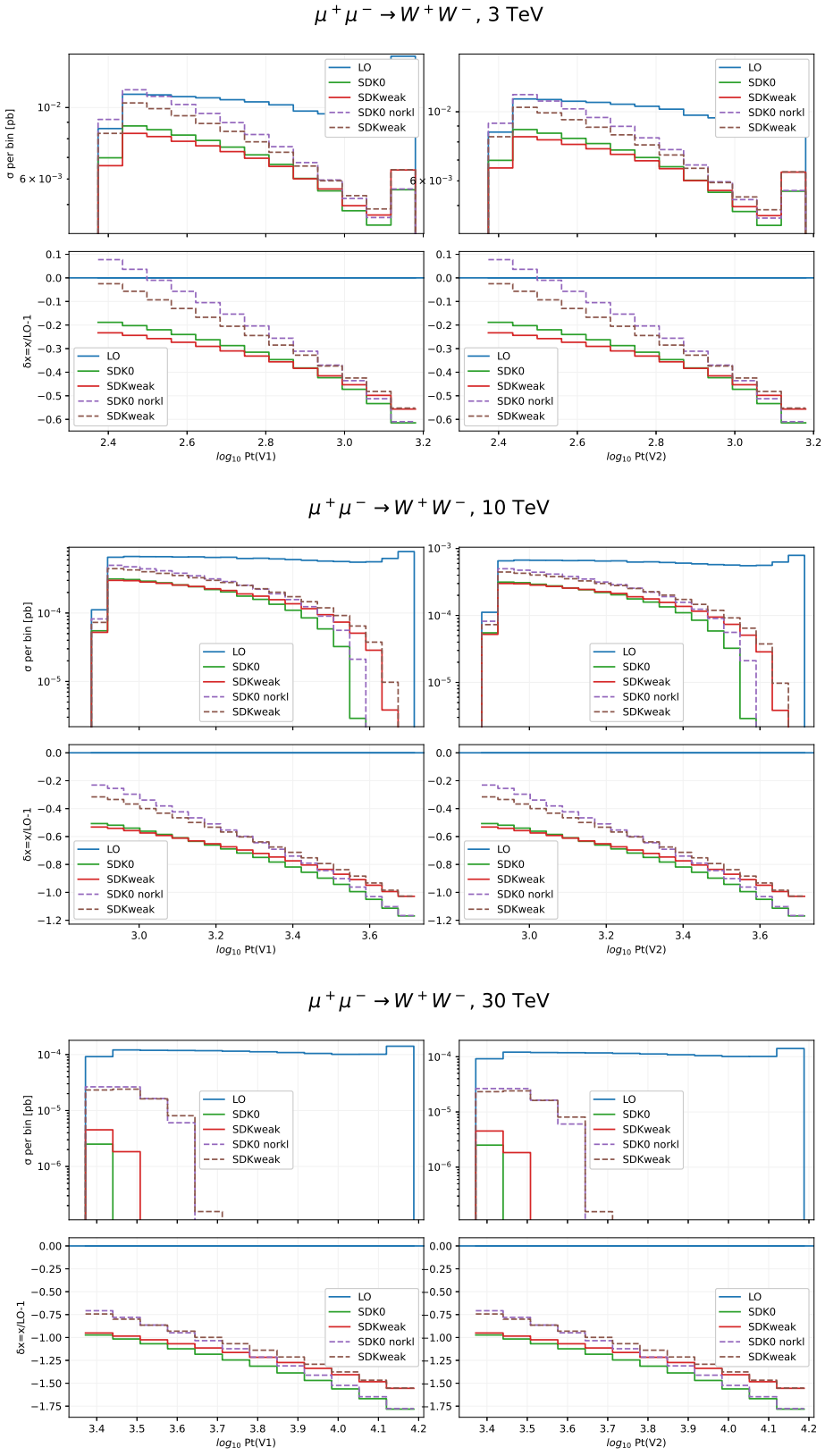

Figure 3.5: Same as Fig.3.4 but for W^+W^- production

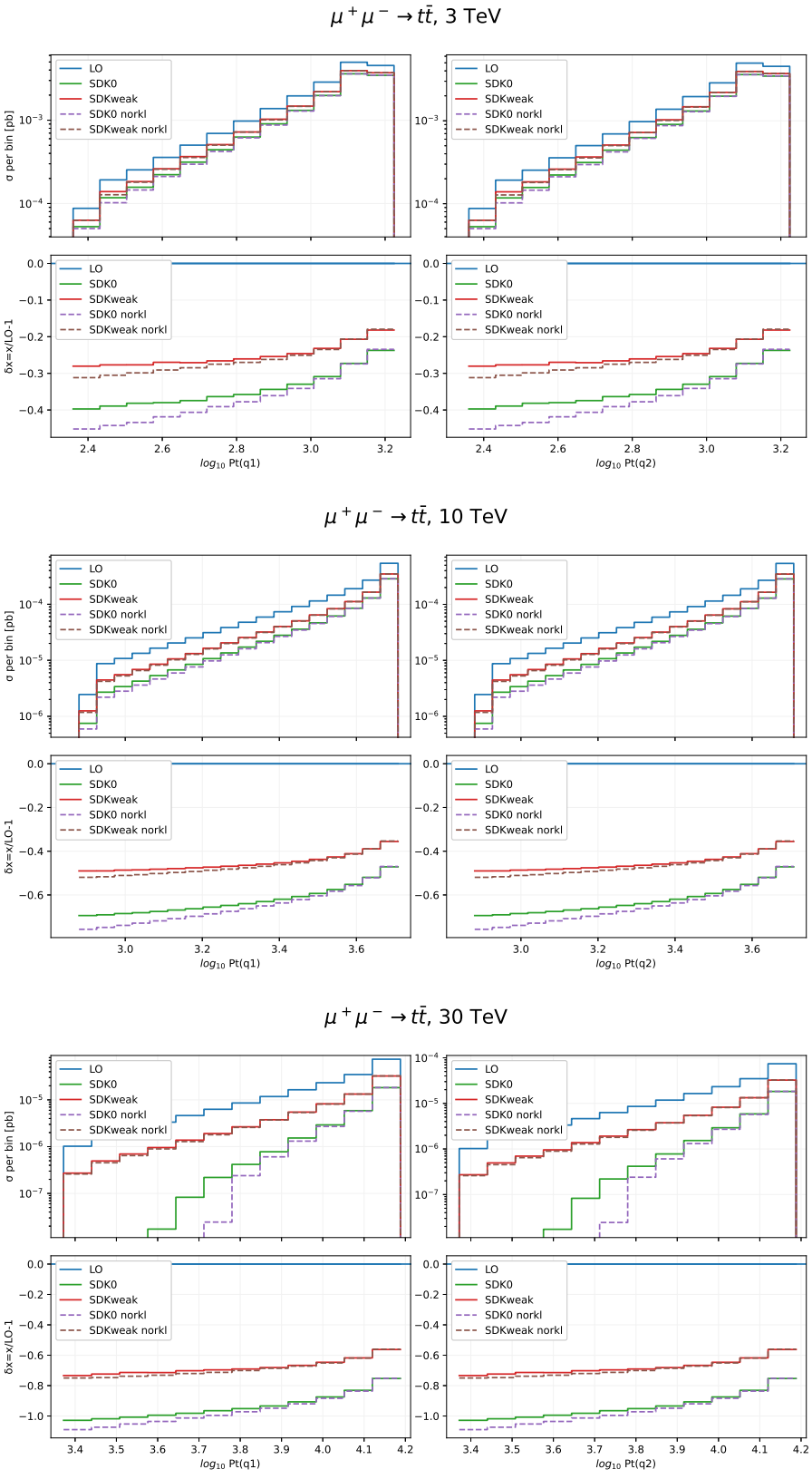

Figure 3.6: Same as Fig.3.4 but for $t\bar{t}$ production

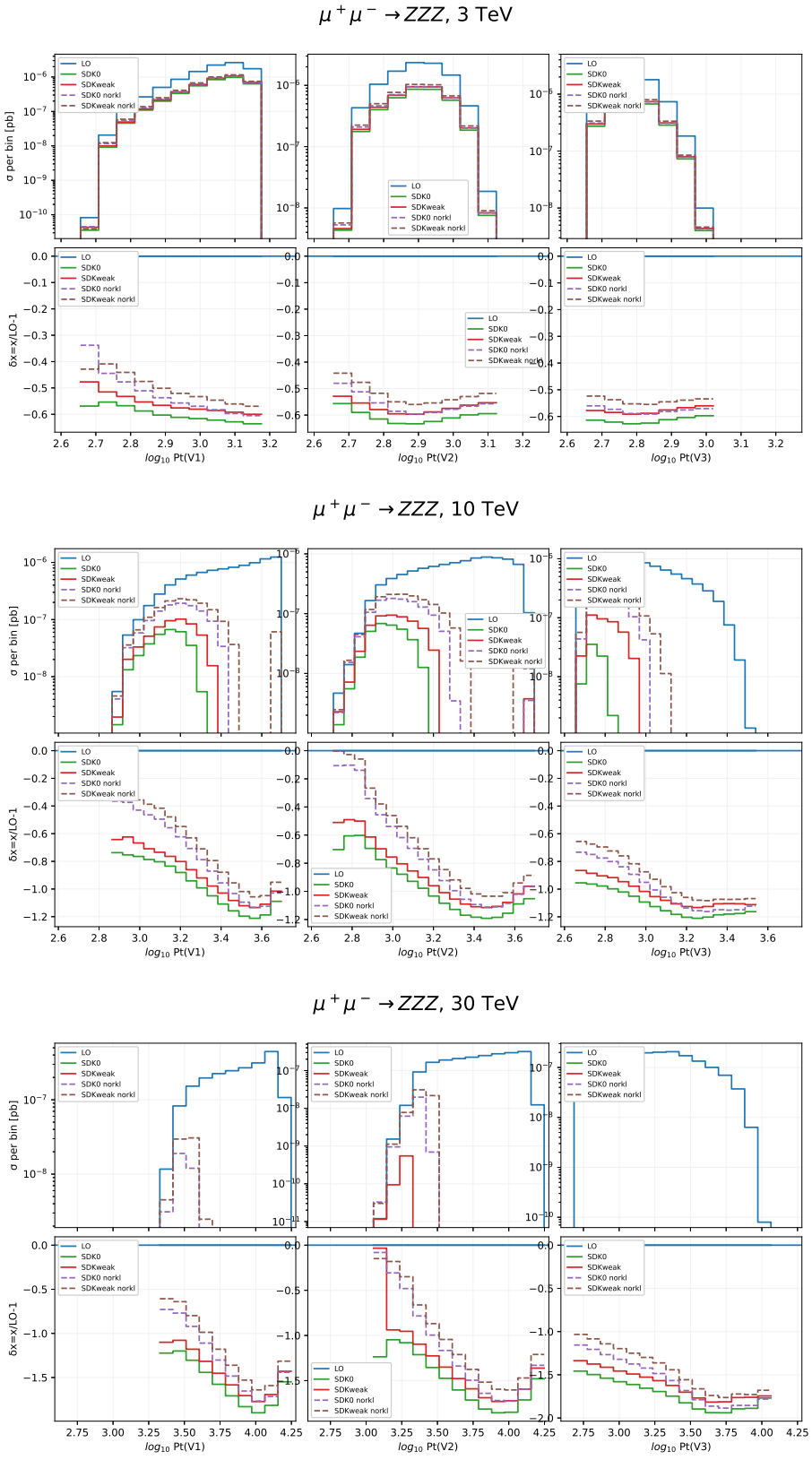

Figure 3.7: Same as Fig.3.4 but for ZZZ production

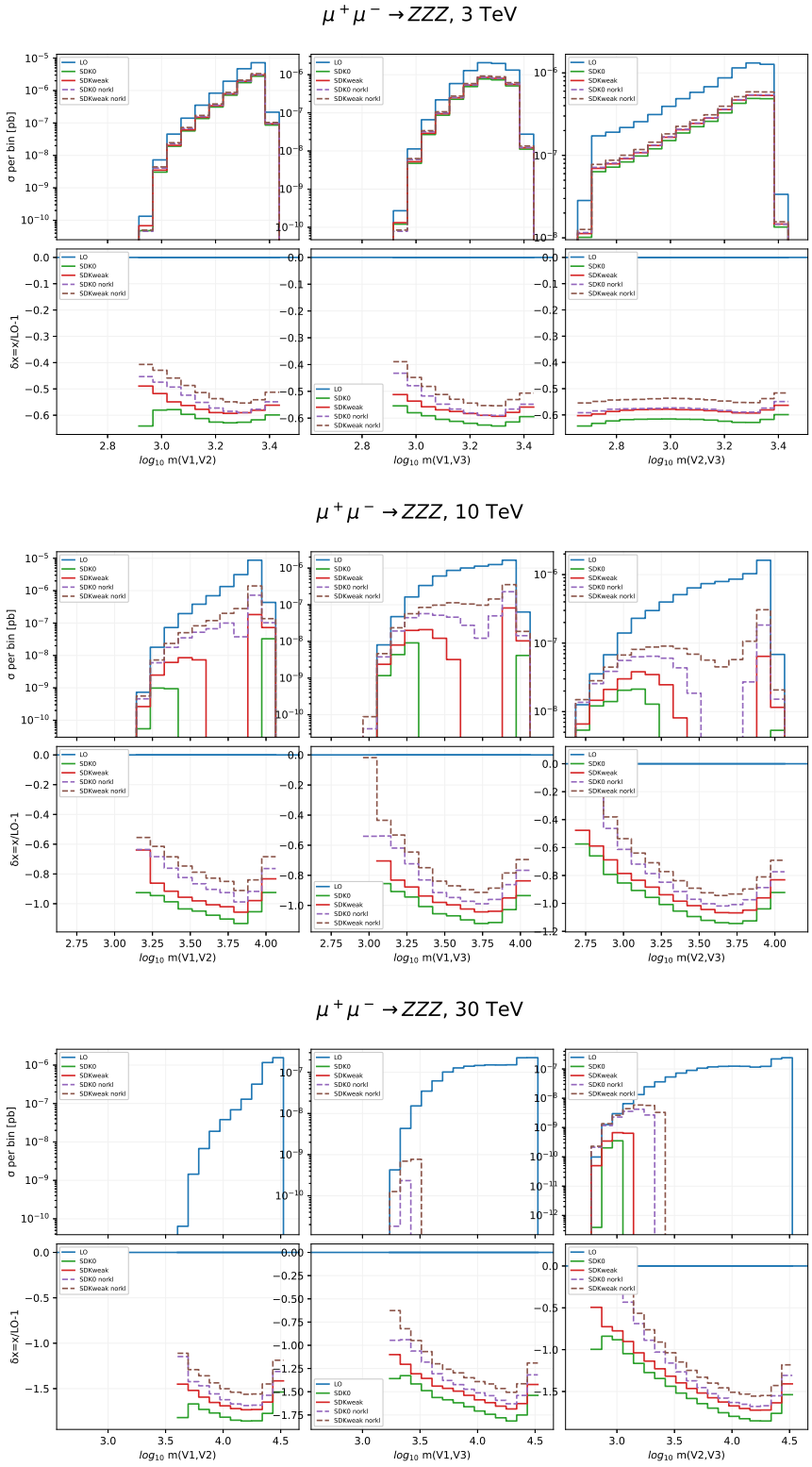

Figure 3.8: Same as Fig.3.7 but w.r.t. the invariant mass of all possible pairs of products

For the process $\mu^+\mu^- \to W^+W^-$, in Fig.3.5 we see a different behavior of the LO cross section but a similar trend for the Sudakov corrections. These bring instantly, at low energy, except for the SDK0 approach without $SSC^{s\to r_{kl}}$ factor, negative contributions. Those with the term $SSC^{s\to r_{kl}}$ active goes, in low p_T region and with the increase of energy, from $\sim -23\%$ to $\sim -97\%$ the value of LO.
In the high p_T region they start, at 3 TeV, bringing $\sim$ -60% of LO, at 10 TeV they reach $\sim$ -120% and at 30 TeV a value of $\sim$ -180% the LO one.
As in the previous process, the approaches without angular factor just differ from the ones with it for low p_T, where they give contributions slightly less negative, but meeting their counterpart in the high p_T zone.

For $\mu^+\mu^- \to t\bar{t}$, in Fig. 3.6 we see that Sudakov corrections show a total different behavior, in all approaches, they become less and less negative with the growth of p_T.
In low p_T region at 3 TeV, where the solid lines are near the $\sim$ -30/40% of LO they reach $\sim$ -20% in high p_T zone at the same energy. At 30 TeV these values goes from $\sim$ -70/100% to $\sim$ -75/60%. In addition, this is the only process where the most negative contributions are the ones coming from the dashed lines, meaning the procedure that does not include the $SSC^{s\to r_{kl}}$ term.

In the last process, $\mu^+\mu^- \to ZZZ$, in Fig. 3.7, we appreciate a similar trend to the one of Fig. 3.5; here Sudakov contributions bring, from the beginning, large negative corrections w.r.t. the LO value. In the low p_T region, as before, the solid and dashed lines are well separated with a decreasing distance between them as p_T grows. The biggest negative contribution are always brought by the solid lines and their difference in low p_T region increases with the increase of energy, from $\sim$ -34% to $\sim$ -120%; the most negative contributions are not the ones at the highest value of p_T but slightly before this region, especially for the hardest Z boson; they reach, starting from 3 TeV up to 30 TeV, values of $\sim$ -63% to $\sim$ -190% the LO one. In Fig.3.8 we can see an interesting fact: Sudakov corrections become, in absolute value, bigger than the LO value and start to decrease after a certain value of transverse momentum to return lower than LO.

3.3.2 Total Cross Sections

Now we will consider the case of total cross section. In the following tables, we will report the values of total cross section for all the previous process and at the same various energies. We will look also the ratio between the total value of the cross section obtained through the different approximations methods and the LO value. The notation used here for specifying the various approximation approaches is inclusive of the LO value and the Sudakov corrections.
When occurs that the values of NLO EW predictions are negative, this means that at this order we cannot obtain a sensible prediction and to obtain a physical result resummation should be performed; we still reported the data to appreciate the magnitude of the correction.

Cross Section (pb)			
	3 TeV	**10 TeV**	**30 TeV**
LO	1.16e-02	1.04e-03	1.16e-04
SDK0/LO	0.94	0.78	0.57
SDK0 norkl/LO	0.96	0.81	0.60
SDK$_{weak}$/LO	0.99	0.90	0.78
SDK$_{weak}$ norkl/LO	1.0	0.92	0.80

Table 3.1: Total cross sections for $\mu^+\mu^- \to e^+e^-$ and the ratio with the different approximations, with $SSC^{s\to r_{kl}}$ on and off.

Cross-Section (pb)			
	3 TeV	**10 TeV**	**30 TeV**
LO	1.88e-02	1.69e-03	1.88e-04
SDK0/LO	0.70	0.45	0.16
SDK0 norkl/LO	0.70	0.44	0.15
SDK$_{weak}$/LO	0.78	0.59	0.38
SDK$_{weak}$ norkl/LO	0.77	0.59	0.38

Table 3.2: Same as Tab. 3.1 but for $t\bar{t}$ production

Cross Section (pb)			
	3 TeV	**10 TeV**	**30 TeV**
LO	1.35e-01	1.21e-02	1.35e-03
SDK0/LO	0.65	0.22	-0.32
SDK0 norkl/LO	0.77	0.34	-0.20
SDK$_{weak}$/LO	0.64	0.26	-0.22
SDK$_{weak}$ norkl/LO	0.74	0.35	-1.12

Table 3.3: Same as Tab. 3.1 but for W^+W^- production

Cross Section (pb)			
	3 TeV	**10 TeV**	**30 TeV**
LO	9.77e-06	9.41e-06	2.05e-06
SDK0/LO	0.38	-0.07	-0.66
SDK0 norkl/LO	0.41	0.08	-0.47
SDK$_{weak}$/LO	0.41	0.006	-0.55
SDK$_{weak}$ norkl/LO	0.46	0.15	-0.34

Table 3.4: Same as Tab. 3.1 but for ZZZ production

Looking at the dimensional analysis of the total cross section, $\sigma \sim \frac{1}{s}$, we see that it decreases with the increase of the energy; for the first three processes, meaning the $2 \to 2$ ones, it descends off of two orders of magnitude; the reason is that for process like $\mu^+\mu^- \to e^+e^-$, at LO the only invariant entering the calculations is s and so, the bigger it is, the smaller become the cross section. The same occurs for the production of top quarks. For $\mu^+\mu^- \to W^+W^-$, in LO calculations enters also a diagram with just a t channel, but there are two with just an s channel, and the same trend is followed.
In the $2 \to 3$ process, $\mu^+\mu^- \to ZZZ$, the fall of the cross section value is not as fast as in the other processes, it is present, but the cross section remains for the three energies always of the same order; this is due to the fact that in this process, at LO in the diagram expansion, appear a dominant number of diagrams with other invariants r_{kl} w.r.t. the number of those with just a s channel.
As said before, all the quantities in the numerator are inclusive of also the LO value; all ratios are smaller than 1 meaning that the approximation contributes with a negative value, apart in one occasion, in Tab.3.1, at 3 TeV with the approach SDK$_{weak}$, where, without angular factors, the ratio not approximated is slightly bigger than 1. In all the processes, as energy grows, the contribution carried from the Sudakov approximations always become more and more negative; this is more evident in the processes of bosons production, where, as seen in the plots for differential distribution, they became in absolute value bigger than the LO part.

3.4 HBR-Heavy Bosons Radiation

In this section, we look at the same previous processes, but in addition we consider the real emission of a Z boson; we will look whether this leads to the partial cancellation between the real emission part and the corresponding virtual one. As already mentioned, while the photon and gluon emission and real radiation of light quarks are necessary to obtain IR-finite predictions of physical observables, the radiation of a heavy boson is not necessary to it, indeed the emission of a heavy particle is considered as a different physical process, so when the HBR (Heavy Boson Radiation) occurs, the cancellation with its virtual counterpart is partial and dependent on the set-up of the observable.
Now we generate the same previous processes at the same energies and cuts with the option available in MadGraph [LOonly], with in addition the emission of a Z boson but ignoring its kinematics, meaning not imposing cuts on it, to see how much of the logarithms coming from loops are canceled by the contribution coming from the emission of a Z boson.

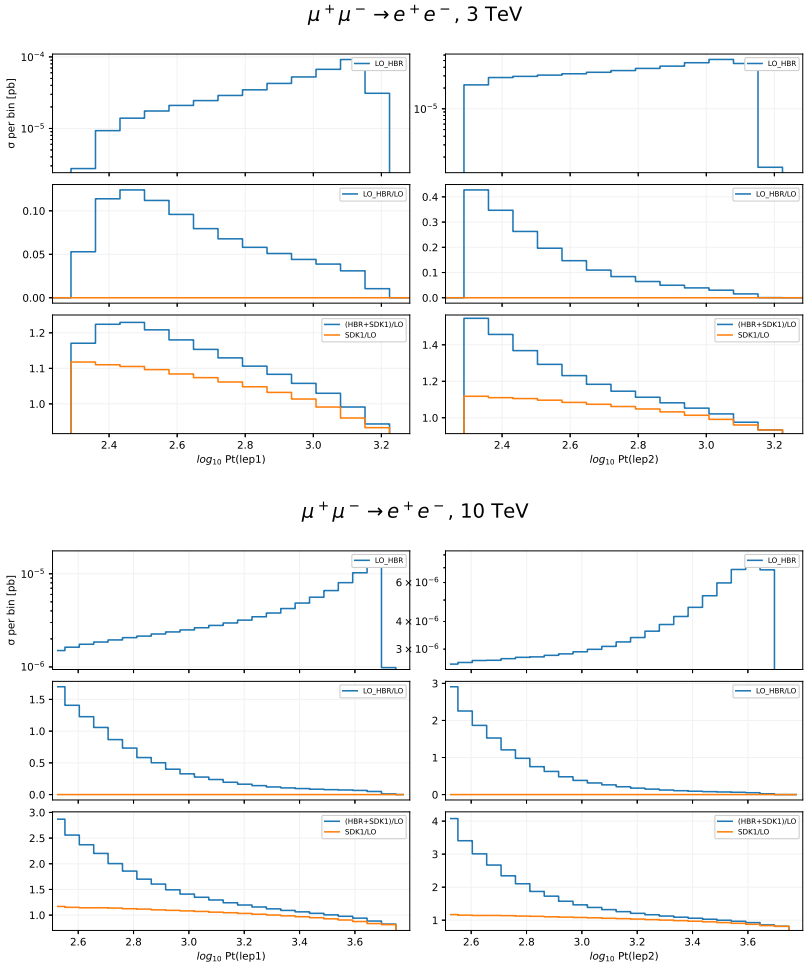

Figure 3.9: At 3 and 10 TeV, for $\mu^+\mu^- \to e^+e^-$ process, in descending order: differential cross section for the process, ratio of the LO HBR cross sections and the LO of the process without HBR, combinations to see the cancellation between real emission and loop counterpart

Here we will present the result at the energies of 3 and 10 TeV for the outgoing particles ordered w.r.t. their hardness. The layout of the plots presents in the upper charts the differential distributions for the process with the emission of the Z boson, in the middle one is plotted the ratio between the differential distributions with and without HBR, that we will call respectively in the text HBR and LO; the lowest charts will have the plot of two ratios: one, the Sudakov approximation SDK_{weak} with the LO curve of the process and the other the ratio between the sum of Sudakov SDK_{weak} approach and the HBR, with the LO. For this analysis, we included the presence of the $SSC^{s\to r_{kl}}$ term in the Sudakov approximation.

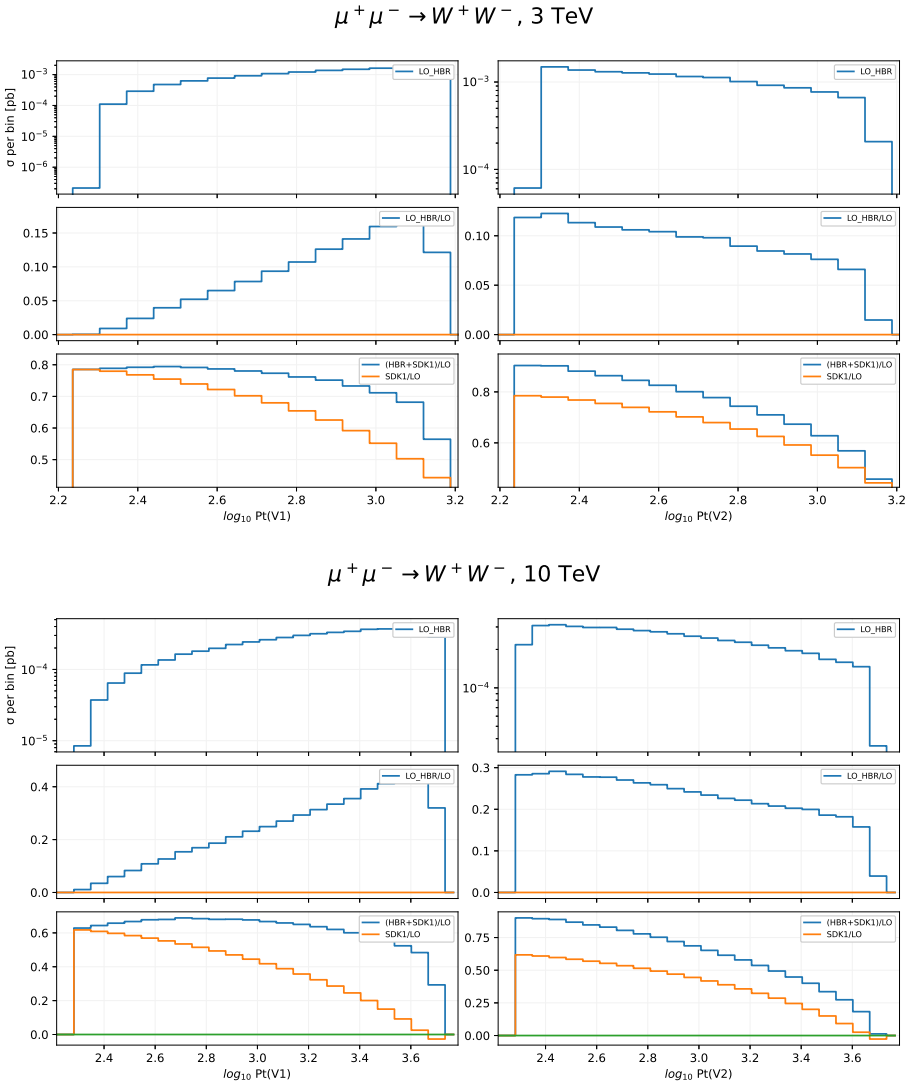

Figure 3.10: Same as Fig.3.9 but for W^+W^- production

Concerning the total cross section, for $\mu^+\mu^- \to e^+e^-$ there is a difference of about two order of magnitude between the process with and without HBR, in favor of the first at 3 TeV, and of one order at 10 TeV; this behavior is not replicated in the other processes where the order of difference of the total cross section is only one for both 3 and 10 TeV. We see that the differential distribution of the process HBR mimics the ones of the process without it. Looking at the second inset of Fig.3.9, it is clear the previous discussed trend, as the ratio, assume a value of order 10^{-2} for the vast majority of p_T values. With the

increase of the energy this ratio became larger, but with the same trend, indeed at 3 TeV the HBR value reaches at most the 10% of the LO in the low p_T region, and descending with the increase of it; at 10 TeV and at low p_T, the HBR value is the 150% of the LO, becoming equal to it at ∼500 GeV and proceeding to decrease. In the third inset, we see that the cancellation between the real emission terms and the Sudakov ones increases; even if the HBR distribution increases with p_T, Sudakov corrections become more and more negative, as shown in Fig.3.4. At 10 TeV this is more evident.
For the $\mu^+\mu^- \to W^+W^-$, the real emission of an extra Z boson does not suppress W production at large p_T like it was happening for the leptons in the previous process considered; at 3 TeV the HBR value reach at most 15% of the LO one and at 10 TeV up to 40%. In the third inset of the two groups of plots about this process, we see that the cancellation become smaller and smaller but at a certain point, toward the highest p_T, starts to become more significant.

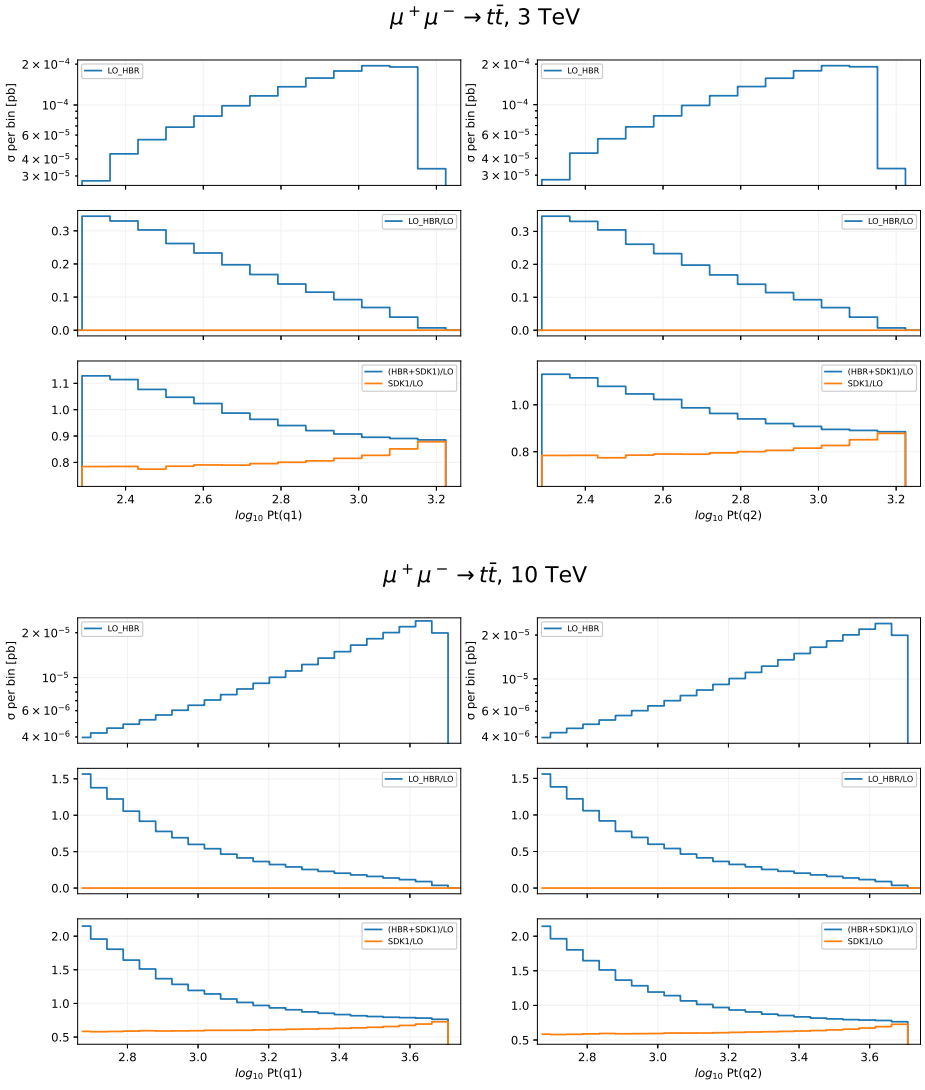

Figure 3.11: Same as Fig.3.9 but for $t\bar{t}$ production

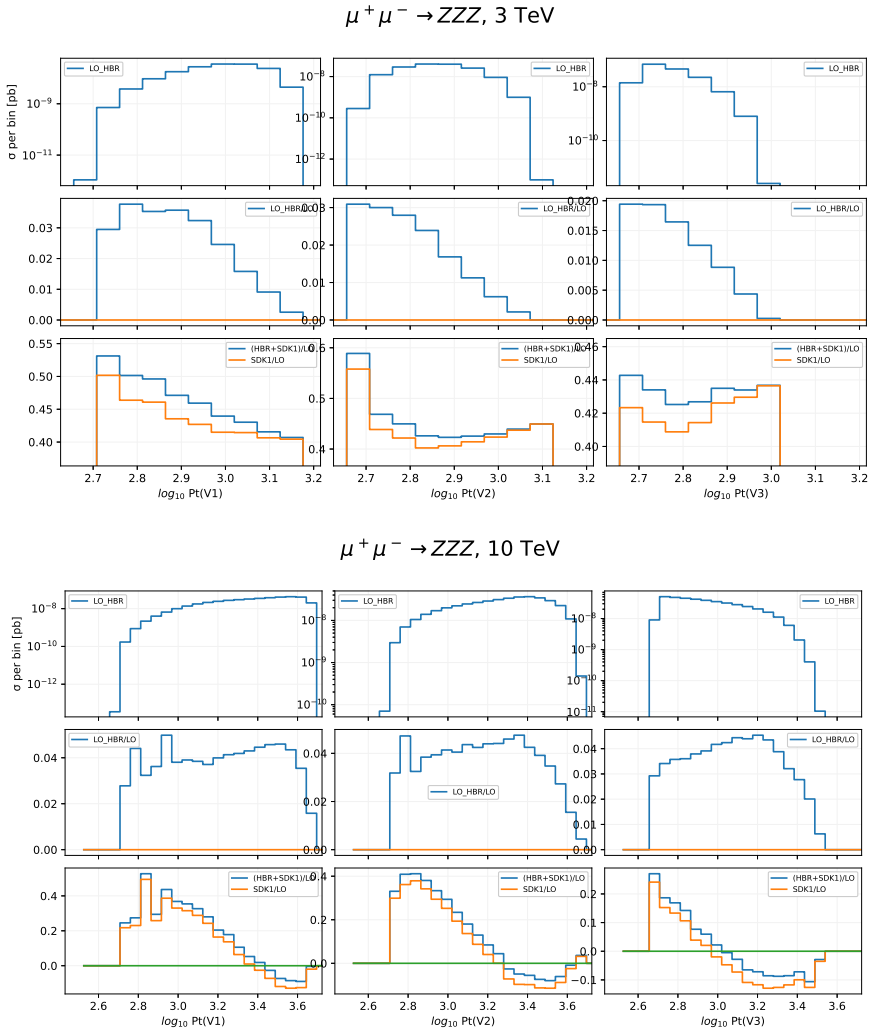

Figure 3.12: Same as Fig.3.9 but for ZZZ production

In Fig.3.11, for $\mu^+\mu^- \to t\bar{t}$, the HBR is more likely to happen at high p_T; at 3 TeV the HBR value reaches 30% of the LO one, decreasing with higher p_T; at 10 TeV the HBR is at most 150% of the LO with a fast dumping as p_T increases. The cancellation happens but is not intense as for the e^+e^- production, also here because the HBR increases with p_T.

For $\mu^+\mu^- \to ZZZ$, in Fig.3.12, we see that the distribution for the HBR is very similar to the one without HBR, as we can see in Fig.3.7, with the HBR differing of some unit percent w.r.t. the LO value for almost all the p_T values. Because of the similar shape of the HBR and LO curve, the shape of the cancellation curve is similar to the first, but with just with a constant shift. With a heavy particle in the final state, high p_T can no more be reached as without it, indeed the highest p_T, is reached when only two particles are produced back to back, but in the case of HBR some energy is required to produce the new particle. Its presence also tends to make the extra particle be produced at low p_T. In general, for a $2 \to 2$ process, adding an extra particle changes the configuration much more than in a $2 \to 3$ process, indeed it changes from having the two particles produced back-to-back to a three body situation, where the back-to-back production is lost. Indeed, the adding of an extra particle in a $2 \to 3$ process, has a more plain impact, being the starting configuration of produced particles already less constrained.

Chapter 4

Conclusions

Fundamental interactions are typically probed at collider experiments, where predictions from the SM are tested against data. A thorough validation or falsification of the SM requires the systematic inclusion of higher-order corrections in theoretical predictions. While at hadron colliders, such as the LHC, such corrections mostly come from strong interactions, at lepton colliders EW corrections play a crucial role. One distinguishing feature of EW corrections is the fact that they grow with the process energy, because of the so-called Sudakov enhancement. In particular, if the proposed muon collider will be funded, the very large operating center-of-mass energy will be such that EW effects will be necessary not for precision physics, but even just to have a reliable estimate of production rates. In this work, we have studied the EW corrections at a muon collider by investigating the dominant contribution originate by Sudakov Logarithms. We have reviewed how these contributions emerge and can be computed, in a way which is considerably simpler with respect to the full EW corrections. Then we have computed the Sudakov-approximated EW corrections for processes at hadron colliders, reproducing existing results. The main result is the computation of such corrections for muon colliders at some benchmark energy values, for a selection of processes. Sudakov corrections. Different approaches have been tried to evaluate the Sudakov corrections: the approach that has been proposed originally by Denner and Pozzorini, as well as some new variants which either better take into account the kinematic structure of the process, or take into account only purely-weak effects. Finally, we have investigated whether these effects, which are of pure virtual origin, are compensated when real emissions of an additional Z boson are considered. We have shown various numerical results, both at the level of total rates and differential distributions, where the impact of the considered corrections can be assessed.

Bibliography

[1] A.Denner, S.Pozzorini, *One-loop leading logarithms in electroweak radiative corrections, [arXiv:hep-ph/0010201v3] (2001)*

[2] Davide Pagani, Marco Zaro, *One-loop electroweak Sudakov logarithms: a revisitation and automation, [JHEP02(2022) 161] (2022)*

[3] Fabio Maltoni, Olivier Mattelaer et al., *Vector boson fusion at multi-TeV muon colliders, arXiv:2005.10289v2*

[4] Hind Al Ali et al. *The Muon Smasher's Guide [arXiv:2103.14043v1]*

[5] C. Aimè et al., *Muon Collider Physics Summary [arXiv:2203.07256v2] [hep-ph] (2022)*

[6] Matthew D. Schwartz, *Quantum Field Theory and the Standard Model*

[7] G. Bell, J.H. Kühn and J. Rittinger, *Electroweak Sudakov Logarithms and Real Gauge-Boson Radiation in the TeV Region, Eur. Phys. J.C 70 (2010) 659 [arXiv:1004.4117].*

[8] R.K.Ellis,W.J.Stirling,B.R.Webber, *QCD and Collider Physics*

[9] Davide Pagani, *Revisitation and automation of one-loop EW Sudakov logarithms, TPP Seminar (2022)*

[10] J. Alwall et al., *The automated computation of tree-level and next-to-leading order differential cross sections, and their matching to parton shower simulations, [JHEP 07 (2014) 079] [arXiv:1405.0301]*

[11] M. Roth and A. Denner, *High-energy approximation of one loop Feynman integrals, Nucl. Phys. B 479 (1996) 495 [hep-ph/9605420] [INSPIRE]*

[12] M.E. Peskin and D.V., Schroeder *An Introduction to Quantum Field Theory. Westview Press*